An inventory of phreatomagmatic volcanoes in the Trans-Mexican Volcanic Belt

Mélida Schliz-Antequera[1*], Claus Siebe[1], Sergio Salinas[2], Geoffrey Lerner[3]

[1]*Departamento de Vulcanología, Instituto de Geofísica, Universidad Nacional Autónoma de México, Coyoacán, C.P. 04510, Ciudad de México, México*

[2]*Colegio de Geografía, Facultad de Filosofía y Letras SUAyED, Universidad Nacional Autónoma de México, Coyoacán, C.P. 04510, Ciudad de México, México*

[3]*Earth Observatory of Singapore, Nanyang Technological University, Singapore*

*Corresponding author: melida.schliz@gmail.com

Twitter: @MelSchliz

March 19, 2024

This manuscript is a non-peer previewed preprint submitted to Journal of Volcanology and Geothermal Research. Please note that the manuscript is currently under review and has not yet been accepted for publication. Subsequent versions of this manuscript may have different content. If accepted, the final version of this manuscript will be available via the 'Peer-reviewed Publication DOI' link on its EarthArXiv web page. Please feel free to contact us with any comments or feedback about our study

Abstract

The formation of phreatomagmatic volcanoes (PVs) usually involves small volumes of magma but also very violent eruptive activity. Along the Trans-Mexican Volcanic Belt (TMVB) the basic conditions that favor water-magma interaction are provided by the presence of frequent small-volume monogenetic volcanism and several inter-montane lacustrine basins. The TMVB is a Plio-Quaternary continental volcanic arc dominated by >3000 monogenetic volcanic structures with only ~3% being the result of phreatomagmatic eruptions. Around 70% of these are clustered in three specific areas within volcanic fields in Valle de Santiago, Serdán-Oriental, and Los Tuxtlas. Here we investigate the low frequency of PVs and their selective locations and whether local environmental conditions play an important role in their formation. An inventory of 103 PVs within the TMVB has been compiled, including tuff cones, tuff rings, and maar-diatremes. The inventory contains morphometric parameters for each structure along with data regarding geological (internal) and environmental (external) parameters of the areas where the PVs are built. The magmatic flux is the first-degree influence in the formation of PVs. Different combinations of environmental parameters have a secondary-degree influence which varies spatially and temporally related to paleoclimate, hydrology, and hydrogeology. A couple of environmental parameter sets are met more often, reflected in the areas with clustered PVs, but less frequent sets of parameters are also detected, reflected in the scattered PVs. Morphometric correlations allow for a clear differentiation between the group of tuff cones and the group of maar-diatremes and tuff rings. In both groups elongated and compound shapes are more frequent.

Very often, human settlements are built around or inside PVs. However, their shapes and relatively small size can be misguiding regarding the hazard that this type of volcanism represents, especially in the absence of knowledge about the conditions that result in these type of eruptions. This inventory allows for the study of the many different conditions and places in which a phreatomagmatic eruption could occur, providing a better base of information to prepare for future eruptions.

Keywords: phreatomagmatic, Trans-Mexican Volcanic Belt, monogenetic, distributed volcanic fields

1. Introduction

Phreatomagmatic eruptions are a type of hydrovolcanism that occurs when a small batch of magma and groundwater, or water-saturated sediments, interact generating a highly explosive eruption (Smith and Németh, 2017; Németh and Kósik, 2020). Phreatomagmatic deposits have been identified in eruptions of complex volcanic systems like stratovolcanoes (Barberi et al., 1989; Cole et al., 1995) and calderas (De Rita et al., 2002; Palladino et al., 2015; Pedrazzi et al., 2019), as well as in the base of scoria cones (Lorenz, 1986; Houghton and Schmincke, 1989). However, volcanoes built predominantly by phreatomagmatic deposits, such as maar-diatremes, tuff rings, and tuff cones (Morrisey et al., 2000), are usually linked to small-volume distributed volcanism, where water has a stronger influence on the eruption dynamic (McGee et al., 2015; Németh and Kósik, 2020).

Phreatomagmatic volcanoes (PVs) present a wide range of compositions, shapes, architectures, and occur in a variety of environmental and tectonic settings (Németh and Kereszturi, 2015; Graettinger, 2018). These structures are after scoria cones the most common volcanic landforms (Fisher and

Schmincke, 1984; Lorenz, 2007) and can be also found associated with any type of volcanic system, clustered as part of distributed volcanic fields and, in a few cases, completely isolated (Ross et al., 2017; Graettinger, 2018). However, the observed population of PVs in volcanic fields tends to be very small compared to other magmatic structures; only in few cases do PVs reach a couple of tens of structures, regardless of the size of a volcanic field or the number of volcanoes contained (Graettinger, 2018). In volcanic fields related to subduction the observed PV population is variable, representing <2% (17) of ~900 monogenetic volcanoes in the Central Andes, Northern Chile (Ureta et al., 2020), but up to ~32% (29) of 91 monogenetic volcanoes in the Lamongan volcanic field, Indonesia (Carn, 2000), and ~27% (8) of 30 monogenetic structures in the Nejapa-Miraflores volcanic field, Nicaragua (Avellán et al., 2012).

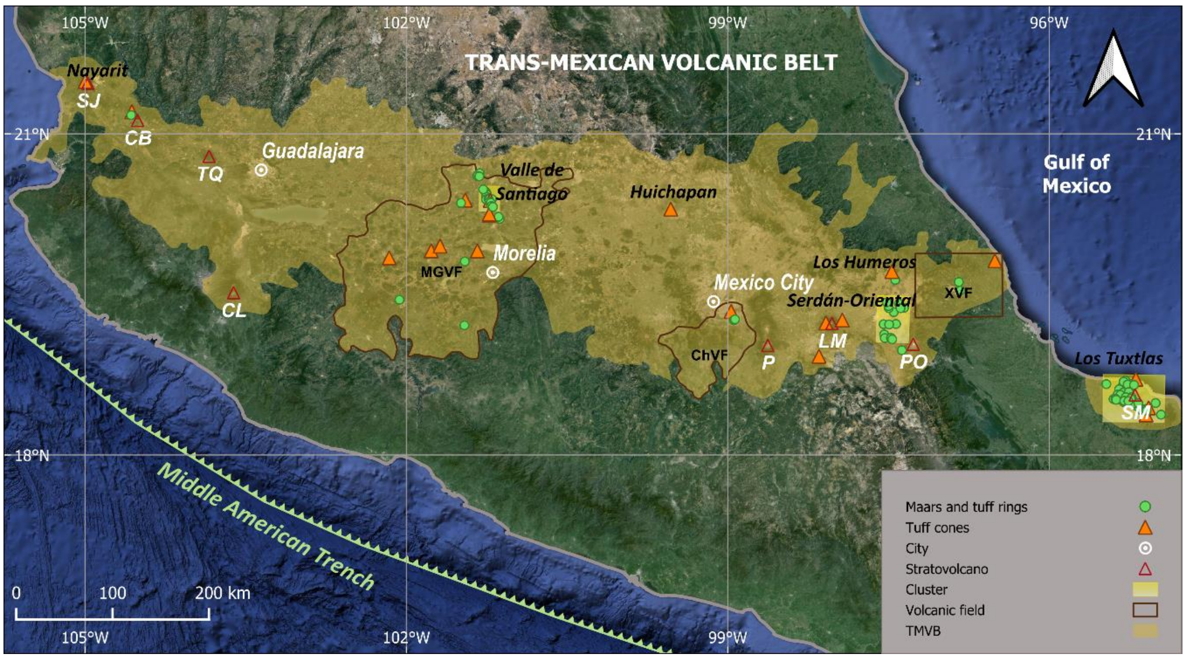

Fig 1. Location of the Trans-Mexican Volcanic Belt and the phreatomagmatic volcanoes listed in the inventory (Table 1). Monogenetic volcanic fields: MGVF= Michoacán-Guanajuato, ChVF= Chichinautzin, XVF= Xalapa. Stratovolcanoes: SJ= San Juan, CB= Ceboruco, TQ=Tequila, CL=Colima, P=Popocatépetl, LM=La Malinche, PO=Pico de Orizaba; SM=San Martín Tuxtla.

The Trans-Mexican Volcanic Belt (TMVB) is an east-to-west, >1000-km-long, Plio-Quaternary continental volcanic arc developed as a result of the subduction of the Rivera and Cocos plates beneath the southern edge of the North America plate (Ferrari et al., 2012). Along the TMVB (**¡Error! No se encuentra el origen de la referencia.**) there are several volcanic fields and important calderas and stratovolcanoes, but this volcanic arc is peculiarly dominated by small-volume monogenetic volcanoes, with >3000 scoria cones (Guilbaud et al., 2012; Siebe and Salinas, 2014). Intra-montane tectonic basins occupied by shallow lakes are common along the volcanic arc. PVs also occur in the TMVB, however, their frequency is lower than what could be expected, representing <3% of all monogenetic structures (Siebe and Salinas, 2014). They are also not evenly distributed along the arc and their occurrence is limited to a few areas that seem to provide the proper conditions required for their formation.

Environmental factors can influence a monogenetic eruption due to the small magma volume involved and short eruption duration (Kereszturi et al., 2011; McGee et al., 2015; Németh and Kereszturi, 2015). Therefore, the understanding of these eruptions also requires the consideration of external factors (pre-existing topography, substrate, hydrogeological conditions, and climate), alongside the internal factors (magma composition, magmatic flux, etc.). The occurrence of this violent type of volcanism in such a variety of conditions represents a need to understand the parameters that favor phreatomagmatism. In that sense, the fields with clustered phreatomagmatic structures represent opportunities to study the poorly understood conditions and interaction between the internal and external factors involved in phreatomagmatic eruptions.

Human settlements are frequently built around or quite close to active volcanic areas, and small-volume monogenetic volcanoes are no exception (Siebe and Macías, 2004; Avellán et al., 2012; Le Corvec et al., 2013). Moreover, small-volume monogenetic deposits are usually a valuable resource for economic activities such as tourism and quarrying (Avellán et al., 2012; Delcamp et al., 2014; Albert et al., 2016; Jácome-Paz et al., 2022). In Mexico there are precedents where pre-Hispanic settlements were affected by monogenetic volcanism causing population reduction, abandonment of cities and migration, and sometimes reoccupation and recovery after the eruptions (Santley, 2007; Reyes-Guzmán et al., 2018; 2023; Chédeville et al., 2020; Dorison and Siebe, 2023; Siebe et al., 2023). With the increasing population and economic activities around this type of structures there is higher exposure to volcanic hazards which, in the case of phreatomagmatic eruptions, are amplified by their highly explosive nature (Németh et al., 2012). Hence, understanding the magma-water interaction that causes these eruptions is vital for volcanic hazard and risk assessments, and requires detailed research of PVs (Lorenz, 2007; Kereszturi and Németh, 2012).

In this work, we present an inventory of small-scale monogenetic phreatomagmatic volcanoes along the TMVB (Supplementary file A) in which available information for each structure has been compiled. The aim of this inventory is to assess and summarize the data regarding environment, distribution, and current state of knowledge about the phreatomagmatic volcanoes of the TMVB and to establish future avenues of research.

In regard to the scale of observation and the purposes of this research, some terms have been used to describe the dataset of the PV-inventory and the environment where these structures are located. For clarification, the term “volcanic field” used herein refers to an area where several, frequently tens or even hundreds of volcanic edifices are present, regardless of the type of volcanic system. Also, the volcanic fields mentioned in this text have been referred to as such in previous research, and the same names were kept in this document. The term “cluster” is used herein to refer to a group of PVs that formed within a relatively short time span (hundreds to a few thousands of years) and are located very close to each other within a specific area or volcanic field (e.g., Mahgoub et al., 2017), while the term “isolated” refers to the opposite situation. Our use of these terms has no specific implications in regard to the nature of the magmatic system.

1.1. Phreatomagmatic eruption dynamics

Magma-water interaction has been associated with eruptions of different magnitudes in monogenetic as well as polygenetic volcanic systems (Morrisey et al., 2000). This research is focused on the volcanic structures generated by the explosive magma-water interaction in small-scale volcanoes associated with monogenetic volcanism within the TMVB.

An eruption is considered phreatomagmatic when the main process of magma fragmentation is driven by molten-fuel coolant interaction (MFCI) in which magma and groundwater, or surface water, have a direct interaction resulting in violent explosive eruption dynamics (Sheridan and Wohletz, 1983; Németh and Kósik, 2020). This process implies a cascade of events in which a molten-fuel (magma) makes contact with a coolant (water) with a significantly higher temperature than the homogeneous nucleation temperature of the coolant (Sonder et al., 2018). Upon contact, the superheating of water generates an incredibly fast transfer from thermic to mechanical energy and therefore a fast formation of a vapor film that expands fragmenting the magma and creating potent shock waves that also fragment the surrounding country rock (Wohletz, 1983; Büttner et al., 2002; Sonder et al., 2018). There are several physical processes involved in MFCI which have been investigated using experimental research with diverse instrumental setups (Wohletz, 1986; Austin-Erickson et al., 2008; Sonder et al., 2018). However, there are still many uncertainties regarding the geometry of the contact area between magma and water, energy transfer processes, influence of the viscosity of the magma, and the scale of the experiments.

Experimentally it has been estimated that a water-magma mass ratio between 0.1 and 0.3 is the optimal interval when the conversion of energy is most efficient and a successful MFCI occurs (Wohletz, 1983; Wohletz and Sheridan, 1983). However, considering the dynamics during the eruption, it has also been pointed out that the ratio involves not just the mass but is controlled by the magmatic flux and water flux (Houghton et al., 1999).

To have a phreatomagmatic eruption, the magma flux, the water availability, and the geometry of their contact must be in a fine balance (Németh et al., 2012; Valentine et al., 2017). Even with available water, high rates of magma discharge during the eruption can surpass the environmental conditions and produce a magmatically controlled eruptive activity (Houghton et al., 1999; Gutmann, 2002; Valentine et al., 2017). Phreatomagmatic phases can occur at any moment during the eruption depending on the magma flux variation and water availability and the balance between these two parameters (Geshi et al., 2019).

The low volume of magma involved in monogenetic eruptions gives external environmental factors a stronger influence on eruption dynamics, the resulting type of volcanic structures formed and their types of deposits (Kereszturi et al., 2011; McGee et al., 2015; Németh and Kereszturi, 2015). External factors are related to the water availability, which can be affected by climate, topography, substrate, aquifer geometry, and groundwater flow (Kereszturi et al., 2011; Kshirsagar et al., 2015). The variable interplay between internal and environmental parameters causes different magmatic system behaviors and the display of diverse magmatic fragmentation mechanisms in MVFs. Phreatomagmatic fragmentation is more likely to occur in cycles of low magma output rate, when environmental conditions can have a greater influence, while dominantly gas-driven magmatic fragmentation is more likely to be expected with higher magma output rates (Kereszturi et al., 2011; Németh et al., 2012; Geshi et al., 2019; Németh and Kósik, 2020).

Distribution of monogenetic volcanoes frequently shows some control by basement structural patterns, especially scoria cones and domes (Németh and White, 2003; Gómez-Vasconcelos et al., 2020; Ureta et al., 2020). The analysis of the spatial distribution of volcanoes within MVFs has led to the conclusion that cone alignments are variably controlled by regional and local stress-fields and pre-existing fractures (Le Corvec et al., 2013), and that crust thickness and the maturity of a MVF also play a role in the clustering of vents, especially in extensional regimes (Mazzarini et al., 2010). However, for PVs there are other factors that seem to have a stronger influence on their distribution, including climate, aquifer geometry, water availability, and topography (Nelson and González-Caver, 1992; Kereszturi et al., 2011). PVs are usually formed in lower topographic ground while the magmatic equivalents are more often formed on high ground (Fisher and Schmincke, 1984; White, 1991; Kereszturi et al., 2011).

1.2 Types of phreatomagmatic volcanoes and their deposits

PVs are classified based on their morphology as *maar-diatremes, tuff rings, and tuff cones* (Fisher and Schmincke, 1984; Morrisey et al., 2000; Kereszturi et al., 2011). Maar-diatremes and tuff rings show wide craters and a low topographic expression with outer slope angles of <20° (Lorenz, 1986; White and Ross, 2011), while tuff cones have a positive relief (Wohletz and Sheridan, 1983), with slopes between 10° and 30° (White and Ross, 2011). The crater dimensions of PVs can vary from a few tens of meters to a few kilometers. Maar-diatremes can reach up to ~5 km (Graettinger, 2018) and tuff cones up to 1.7 km in diameter (Wohletz and Sheridan, 1983).

During the formation of a maar *sensu stricto*, the shock waves cut and fragment the pre-existing rock and develop an inverse cone-shaped deep diatreme, hence the name maar-diatreme (Lorenz, 1986). If the maar crater floor has not been filled with sediments, it is possible to observe the pre-existing rock exposed in the inner walls. Tuff ring development is considered to have a shallower explosion locus and therefore involves a shallower excavation (White and Ross, 2011; Kereszturi and Németh, 2012).

The ejecta ring of PVs is formed by sequences of base-surges (Waters and Fisher, 1971; Fisher, 1977), today also called dilute pyroclastic density currents (PDCs, Branney and Kokelaar, 2002), and fallout deposits, with variable thicknesses and clast-sizes ranging from ash to blocks. Base-surge deposits are formed by thousands of thin layers, each caused by one of the multiple shock waves produced by MFCI processes. These deposits are typically poorly sorted, well-laminated, with low-angle cross-bedding and dune structures, as well as ballistic impact sags and U-shaped channels (Fisher, 1977). Their thickness and features are better developed in proximal areas; the thickness of the deposits decreases logarithmically with distance from the vent, and they display planar bedding features and better sorting (Fisher and Schmincke, 1984). Also related to base-surge deposits is the occurrence of vesiculated tuffs and accretionary lapilli that develops during fallout of thin ash in moist conditions (Lorenz, 1974; Fisher and Schmincke, 1984). The type of clast found in these deposits is diverse in shape, grain-size, vesicularity, and texture (Auer et al., 2007; Kereszturi et al., 2011; Avellán et al., 2012). Non-juvenile lithic proportions in tephra rings vary and are at least somewhat dependent on the type of structure. Maar-diatremes can have lithic proportions of up to 90 wt.% (White and Ross, 2011), while for tuff rings proportions from <5% (Lorenz, 1986) to 55% (Houghton and Schmincke, 1989) have been reported. Tuff cones typically have the lowest proportions of non-juvenile content (White and Ross, 2011).

The deposit sequence reflects the style and dynamics, as well as their variation during the eruption (Kereszturi and Németh, 2012). It is common to find PVs with mixed or hybrid features (Houghton and Schmincke, 1989; White and Ross, 2011; Németh and Kereszturi, 2015). The magma-water ratio as well as the depth of interaction are important factors in the resulting structure. Deep level interaction with groundwater and limited water is expected to form maar-diatremes, while for tuff rings and tuff cones the interaction is believed to be shallower (White and Ross, 2011). For the formation of tuff cones abundant water is expected. Therefore, magma-water ratios vary for each type of structure, with a ratio of 0.3 associated with the highest values of explosive energy in experiments (Sheridan and Wohletz, 1981).

1.4. Tectonic setting

The subduction-related TMVB (**¡Error! No se encuentra el origen de la referencia.**) has an east to west direction and runs 15° oblique to the WNW-ESE-oriented Middle American Trench (MAT) in the Pacific (Pardo and Suárez, 1995). It is ~1000 km long and covers an area of ~160,000 km^2, crossing the central area of Mexico from the Gulf of California in the west to the Gulf of Mexico in the east. The variations in the geometry and subducting angle of the slab beneath the TMVB are believed to be the cause of the variation in its width (between 90 and 230 km) and its oblique position with respect to the MAT (Pardo and Suárez, 1995; Ferrari et al., 2012). The crust thickness under the TMVB is 50 km in the east and gets thinner towards the west (≤40 km) (Ferrari et al., 2012).

The TMVB is located in a complex area covering different tectonostratigraphic terranes, which are heterogeneous in age and lithology and comprise the basement of this volcanic arc (Pasquaré et al., 1987). Furthermore, in the building process of the TMVB, pre-existing fault systems have been reactivated and increase the complexity of the dynamic along the arc (Ferrari et al., 2012). One of the proposed reactivated systems strikes north to south and has been related to the extension of the Basin and Range province and the formation of grabens and horsts that subsequently turned into intermontane tectonic basins where shallow lacustrine environments developed and are common within the TMVB (Pasquaré et al., 1987; Henry and Aranda-Gómez, 1992). Several PVs are located at the margins of some of these tectonic basins (Siebe and Salinas, 2014). Currently, the stress-regime and deformation in the TMVB is extensional, and the extension is higher in the W part of the arc (Suter et al., 2001; Ferrari et al., 2012).

Along the TMVB are several volcanic fields, important calderas, and stratovolcanoes, but the arc is dominated by small-volume monogenetic volcanoes with >3000 visible structures (Guilbaud et al., 2012; Siebe and Salinas, 2014). The beginning of MVFs along the arc has been linked to the latest phase of the TMVB in which roll-back of the subducting slab has supposedly influenced the migration of the volcanic front and the development of extensional faulting since around 5 Ma (Ferrari et al., 2012).

2. Methodology

The identification of PVs within the TMVB for integration into the inventory was made through literature review and visual recognition using satellite images and maps. Literature review considered scientific articles, theses, reports, and maps. Some structures without published information were confirmed on the ground during fieldwork of other research projects. The type and quality of information varies significantly between structures. Some have not been previously recognized as PVs, and most of them have not been investigated in detail, hence for many structures data is not available.

When possible, the information gathered comprises geological data about the structure such as edifice volume, geochemistry, faulting, radiometric dating, and eruption dynamic. Environmental parameters were gathered from various sources: data regarding hydrogeological conditions were consulted in CONAGUA reports from 2020 (https://sigaims.conagua.gob.mx/dma/acuiferos.html), and climate information was acquired from a network of climate monitoring stations and records since 1950 (https://smn.conagua.gob.mx/es/climatologia/informacion-climatologica/informacion-estadistica-climatologica).

2.1. Morphometric analysis

The initial stage of the morphometric analysis involved evaluating the preservation state of each PV. To assess the morphological preservation state, we adopted the criteria utilized in the Maar Volcano Location and Shape (MaarVLS) database (Graettinger, 2018). According to these criteria, a PV would be considered preserved if at least 75% of the tephra ring volume remained intact. In determining the location (coordinates and altitude) and morphometric parameters, we employed Google Earth tools whenever the preservation state of the structures permitted. Specifically, Google Earth 3D and elevation profile tools were utilized to measure crater diameter, height, depth, and direction of maximum elongation, with changes in terrain inclination serving as reference points.

The parameters were determined through the following measurements: maximum height (MaxHeight), average height (AvHeight = Hco), depth, maximum and minimum crater diameter (MinCrD and MaxCrD), average crater diameter (AvCrD = Wcr), maximum and minimum cone diameter (MinCoD and MaxCoD), average cone diameter (ACVoD = Wco), perimeter (P), and crater area (A).

The dimensional ratios calculated include the aspect ratio (AR), elongation (EL), and isoperimetric circularity (IC), which were determined using the equations provided in Graettinger (2018). Additionally, the ratios Hco/Wco, Hco/Wcr, and Wcr/Wco were calculated, where Hco represents the average cone height, Wco represents the average cone diameter, and Wcr represents the average crater diameter (Wood, 1980).

2.2. Statistical analysis

The inventory comprises both categorical and continuous types of data. Categorical data provide information about environmental and magmatic system features. To analyze this type of data, contingency tables have been employed, enabling the understanding of the distribution of environmental features in relation to each other.

The continuous data type consists of measured values for morphometric parameters and certain environmental entries (e.g., precipitation and temperature). Statistical descriptors were computed for these specific sub-sets of data. It was not feasible to measure certain morphometric parameters for several PVs (e.g., for some structures average crater diameter or height could not be confidently determined). As a result, the number of structures included in the calculation of statistical descriptors varies across different variables and sub-sets. For instance, in certain cases, only the maximum crater diameter may be measured, resulting in a higher number of structures available for analysis based on these parameters compared to the average crater diameter, which might have fewer recorded entries. Groups considered to have insufficient data are not described.

The frequency distribution analysis revealed that the data does not follow a parametric distribution, non-normal distribution, and a wide range of dispersion for several parameters (**¡Error! No se**

encuentra el origen de la referencia.). Given the statistical behavior observed, the median is considered a more accurate measure of central tendency than the mean value for describing the data, so the median is the value used as the reference statistical descriptor.

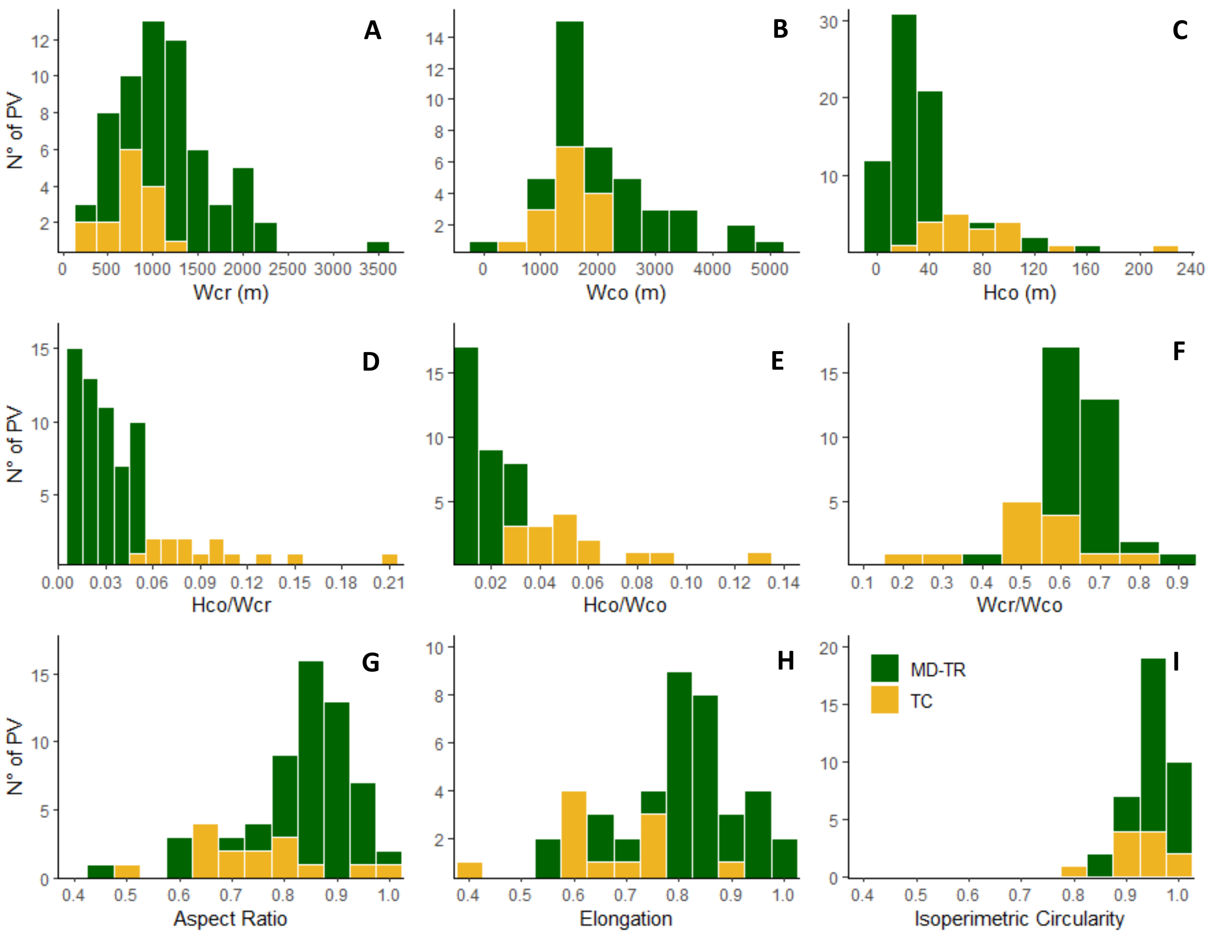

Fig 2. Frequency distribution of morphometric parameters. A) Average crater diameter (Wcr), B) Average cone diameter (Wco), C) Average cone height, D) Hco/Wcr ratio, E) Hco/Wco ratio, F) Wcr/Wco ratio, G) Aspect ratio (AR), H) Elongation (EL), and I) Isoperimetric Circularity (IC).

The parameters of PVs were analyzed separately for tuff cones (TC) and maar-diatremes and tuff rings (MD-TR). The values of the categorical entries were then used as filters to analyze the data within sub-sets. This allowed the evaluation of the morphometry in relation to environmental and magmatic system features. The anomalous morphometric values within the groups were not removed, as they present an opportunity to analyze the potential processes that impact the ideal shape of a PV structure. It is worth noting that because the median serves as the reference morphometric statistical descriptor, the inclusion of anomalous values does not affect the overall outcome.

Although the mean is not used herein as a reference statistical descriptor, the coefficient of variation (CV) can provide valuable insights. The CV is the ratio of the standard deviation to the mean and serves as a measure of data dispersion and uniformity. A lower CV indicates a less dispersed and more uniform dataset. This becomes particularly useful when comparing the dispersion among different datasets, especially when analyzing the morphometry of distinct groups within the inventory.

2.3. Age data

Through literature examination and data gathering, age data were obtained representing various dating methods, radiocarbon dating on paleosol and pollen samples, Ar-Ar, K-Ar, and paleomagnetism. Discrepancies in age results emerged for some structures when comparing Ar-Ar or K-Ar dating with radiocarbon dating. In instances of such divergence, the preferred method for determining age, especially for younger PVs (< 40,000 years BP), was radiocarbon analysis. However, for older structures (> 40,000 years BP) exclusively dated through Ar-Ar and K-Ar methods, these results were considered.

To evaluate the age trend throughout the entire inventory, the different types of dating analyses were considered. Among these, radiocarbon ages held the predominant position in the gathered information. Additionally, stratigraphic correlation contributed to inferring approximate ages. An age map was created to illustrate the primary epochs during which the PVs were formed.

To investigate correlations with environmental parameters, only radiocarbon ages were employed, aligning them with paleoclimate conditions also derived from radiocarbon analysis. All reported uncalibrated radiocarbon ages were calibrated using the IntCal20 calibration curve (Reimer et al., 2020) via OxCal 4.4 (Bronk Ramsey, 2009) for this purpose.

2.4. Data treatment

The decision to include PVs in the inventory was based on field observations and published research, when possible. In some cases, PVs reported in research papers were not included if the information regarding the structure was inconsistent or if there was no evidence of phreatomagmatic activity during field visits. Despite this, several reported structures that could not be confirmed in the field were still included in the inventory, due to lack of sufficient arguments to exclude them.

To achieve consistency in the dataset, the measurement of morphometric parameters followed a standardized approach throughout the entire inventory. Consequently, even if research publications reported morphometric values for certain PVs, those values were not incorporated into the inventory. The aim was to uphold consistency by exclusively relying on the data collected using the established methodology employed across all entries regarding the measuring tools and criteria.

3. Results

The inventory comprises 103 PVs identified along the TMVB. These structures have been classified as maar-diatremes, tuff rings, and tuff cones according to morphological features, field observations, and available published data. Maar-diatremes and tuff rings (MD-TR) display a similar low-surface morphology (Lorenz, 1986) and represent 81% (83) of the dataset, while tuff cones (TC) are more prominent topographic features (Wohletz and Sheridan, 1983) and represent 19% (20).

Table 1. Inventory of PVs showing their number and distribution in volcanic fields along the TMVB and their percentages within each field. Based on data from [a] Hasenaka (1994), [b] Suter et al. (2001), [c] Jaimes-Viera et al. (2018), [d] Chedeville et

al. (2020), [e] Jácome-Paz et al. (2022), [f] Sieron et al. (2021), [g] Verma (2006), [h] Siebe and Salinas (2014), [i] Ferrari et al. (2012), and [j] Andreani et al. (2008).

Volcanic field (VF)		N°of PVs		% Inventory		Vents in VF	% PVs per VF	Area (km^2)	Tectonic setting
Michoacán-Guanajuato	*South of Río Lerma*	*7*	30	*6.80*	29.13	1400[a]	2.1	40000[a]	Subduction / intra-arc rifting[b]
	Yuriria	*4*		*3.88*					
	Valle de Santiago	*14*		*13.59*					
	Irapuato	*3*		*2.91*					
	Huanímaro	*2*		*1.94*					
Sierra de Chichinautzin		3		2.91		227[c]	1.3	-	Subduction / intra-arc rifting[b]
Valsequillo Basin		1		0.97		-	-	-	Subduction / intra-arc rifting[b]
Serdán Oriental		14		13.59		30[d]	46.7	1530	Subduction / intra-arc rifting[b]
Xalapa		3		2.91		72[e]	4.2	-	Subduction / intra-arc rifting[b]
Los Tuxtlas		43		41.75		350[f]	12.3	2200[g]	Subduction/ lateral slip[j]
Strato-volcanoes	*San Juan*	*1*	6	*0.97*	5.83	-	-	-	Subduction / intra-arc rifting[b]
	Ceboruco	*2*		*1.94*					
	Malinche	*2*		*2.91*					
	Pico de Orizaba	*1*		*0.97*					
Calderas	*Huichapan*	*1*	3	*0.97*	2.91	-	-	-	Subduction / intra-arc rifting[b]
	Los Humeros	*2*		*1.94*					
TMVB		***103***		***100.00***		***3000[h]***	***3.4***	***160000[i]***	***Subduction/ intra-arc rifting[b]***

3.1. Location and distribution

PVs are unevenly distributed throughout the TMVB. The structures are located between a minimum altitude of 14 masl and a maximum of 3166 masl, with 75% located below 2144 masl (**¡Error! No se encuentra el origen de la referencia.**a) and can be found in different zones of the TMVB. However, 71 PVs (69%) are clustered, with 14 or more closely spaced phreatomagmatic structures located within volcanic fields in the Los Tuxtlas (LTVF) (41.7%), Serdán-Oriental (SOVF) (13.6%), and Valle de Santiago (13.6%) areas, while 31.1% of the structures are scattered (Table 1, Fig 1).

The PVs-inventory shows that these structures represent 3.4% of monogenetic volcanos in the TMVB, estimated to contain a minimum of 3000 volcanic structures (Guilbaud et al., 2012; Siebe and Salinas, 2014). The percentage of PVs is highly variable between the different volcanic fields of the TMVB, and there is no correlation between the size of an area and the number of volcanoes. The MGVF is the largest of the volcanic fields in this inventory. It covers an area of ~40,000 km^2 (Hasenaka and Carmichael, 1985) and contains the largest amount of monogenetic volcanoes in the TMVB, but PVs only represent 2.2% of the volcanic structures. The LTVF has an area of ~2,200 km^2 (Verma, 2006) and contains the highest number of PVs which account for 12.3% of the total of volcanic vents in this field. In the SOVF there are >30 monogenetic volcanoes (Chédeville et al., 2020) within an area of ~1530 km^2 with PVs representing 46.7% of the total volcanic vents. This is the highest population of PVs related to the volcanic vent population in a specific area within the TMVB. The conditions for the formation of PVs in the TMVB have been met in different types of volcanic systems, however PVs in the inventory are significantly more frequent in MVFs (91%, Table 2). MVFs in which mostly other monogenetic volcano types are present (e.g., MGVF and SOVF) contain 48% of the PVs in the inventory, while MVFs where small-volume structures occur in the lowlands along valleys cutting lava flows from shield volcanoes (e.g., LTVF and XVF) contain ~44%. Only 8.7% of PVs in the inventory are related to composite volcanic systems, where they usually occur scattered and often isolated (6% occur on the lower flanks of San Juan, Ceboruco, and La Malinche stratovolcanoes, while 3% formed near the rims of Huichapan and Los Humeros calderas).

3.2. Preservation state

Fig 3. Satellite imagery taken from Google Earth with examples of modified PVs. A) Lava flow produced at the end of the eruption that formed Potrerillo II tuff ring; B) quarrying, urbanization, and agricultural activities modified Joya Estrada maar; C) natural erosion modified Isla Tanaspi; D) El Caracol tuff cone affected by pre-existing topography of a NE-SW normal fault, and scoria cone on the NW rim of the crater from which lava flows were extruded at the end of the same eruption that produced the tuff cone.

Almost 20% of the PVs are considered preserved. This means that in these structures the shape and most (>75%) of the tephra ring still remain (Graettinger, 2018). This condition was better assessed during the measurement of the morphometric parameters. However, a "preserved" PV could still be affected by a modifier process, and frequently one or more processes are modifying a single structure (Fig 3).

The original geometry of a PV could have been modified by processes occurring during or immediately after the eruption (syn-eruptive) and/or by other processes in post-eruptive times. In some cases, pre-existing topographic features such as fault scarps or scoria cones can impede the formation of a PV structure with an ideal geometry (e.g., Atexcac maar, El Caracol tuff cone). Syn-eruptive processes can also shift the internal and/or external conditions during a phreatomagmatic eruption with sudden switches in eruptive style leading to the subsequent emission of lava flows (Fig 3a), domes, or scoria cones (Fig 3d), which can modify the previously built PV tephra ring by breaching or partially burying. Much later volcanic activity can also modify a pre-existing PV. In many cases information is insufficient to ascertain if a modifying volcanic activity was syn- or post-PV. These cases were grouped in one single category (modified by syn- or post-volcanic activity), which represents 21% of the inventory.

Most post-eruptive processes are usually due to either natural erosion (76%) (Fig 3c), anthropic activity such as quarrying (15%) (Fig 3b), and construction of human settlements and agriculture (23 %). Anthropic activities such as urbanization and agriculture take place either around or inside craters (e.g., Joya de Álvarez in Valle de Santiago).

3.3. Environment

The area covered by the TMVB is vast and contains a diversity of climate and weather conditions. PVs are located in sites with a current minimum annual precipitation of ~350 mm/yr and a maximum of ~4500 mm/yr, with 75% of the PVs occurring in areas with <2490 mm/yr (Fig 4). Half of the PVs (~50%) occur in sites with a precipitation that ranges between 350 and 875 mm/yr. However, according to CONAGUA hydrological data (https://sigaims.conagua.gob.mx/dma/acuiferos.html) >60% of the structures are located above aquifers with a currently negative water balance, where

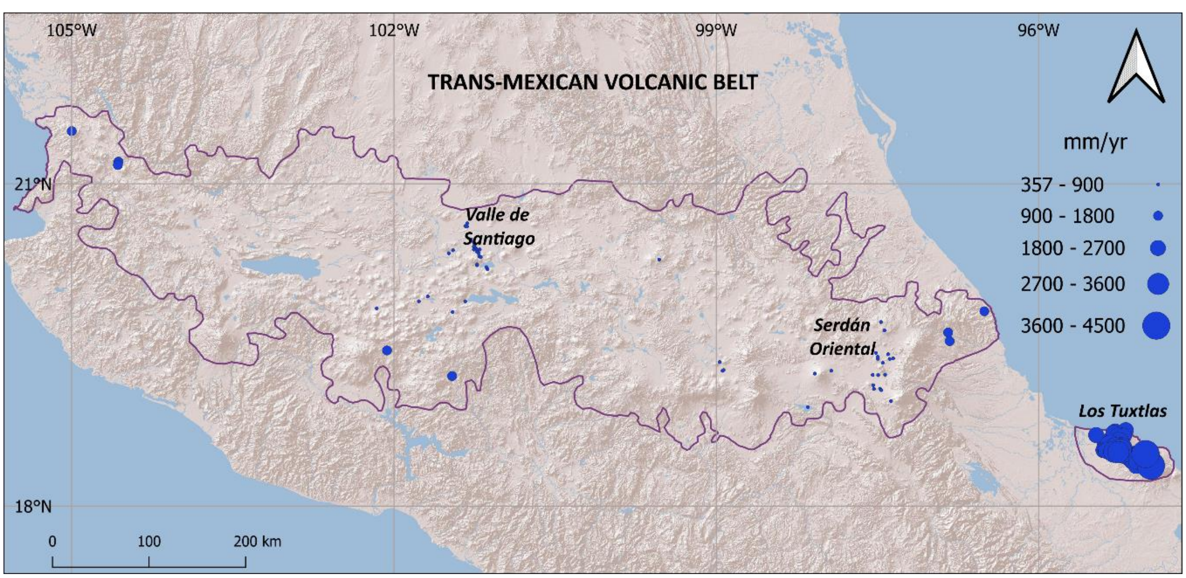

Fig 4. Annual precipitation levels estimated for the period 1950-2012 from the closest weather monitoring station to each PV in the TMVB (CONAGUA, (https://smn.conagua.gob.mx/es/climatologia/informacion-climatologica/informacion-estadistica-climatologica).

evaporation is greater than precipitation and there is excessive groundwater exploitation of the aquifers for human activities. LTVF is one of the few areas within the inventory with a positive water balance and the highest annual precipitation with an average of 2868 mm/yr.

Diversity is also evident in regard to hydrogeological conditions. Approximately 72% of PVs occur within exorheic basins, and 68% of PVs are located in fluvial environments (Table 2). Additionally, 64% of the structures are nested in older lava flows within MVFs and calderas. Lacustrine environments represent 30% of PVs and are also associated with MVFs. Combined host aquifers (granular and fractured material) account for 82% of the sites where PVs occur.

Table 2. Frequency table of PVs by type of structure vs. environmental and internal parameters

Parameter	Inventory		Maar/Tuff Rings		Tuff Cones	
	N	%	N	%	N	%
Inventory	103	100.0	83	80.6	20	19.4
Preserved	20	19.4	13	12.6	7	6.8
Hydrological Environment						
Fluvial	70	68.0	60	58.3	10	9.7
Lacustrine	31	30.1	22	21.4	9	8.7
Litoral	2	1.9	1	1.0	1	1.0
Aquifer Host						
Combined	85	82.5	74	71.8	11	10.7
Hard-Rock	10	9.7	5	4.9	5	4.9
Soft-rock	3	2.9	2	1.9	1	1.0
NA	5	4.9	2	1.9	3	2.9
Basin						
Endorheic	27	26.2	20	19.4	7	6.8
Exorheic	74	71.8	63	61.2	11	10.7
NA	2	1.9	-	-	2	1.9
Age						
Holocene	10	9.7	8	7.8	2	1.9
Late Pleistocene	18	17.5	12	11.7	6	5.8
Early Pleistocene	1	1.0	0	0.0	1	1.0
NA	74	71.8	63	61.2	11	10.7
Volcanic System						
Caldera	3	2.9	1	1.0	2	1.9
MVF	49	47.6	39	37.9	10	9.7
Shield and MVF	45	43.7	41	39.8	4	3.9
Stratovolcano	6	5.8	2	1.9	4	3.9
Juvenile Composition						
Mafic	12	11.7	10	9.7	2	1.9
Intermediate	12	11.7	8	7.8	4	3.9
Felsic	4	3.9	4	3.9	0	0.0
NA	28	27.2	61	59.2	14	13.6

3.4. Composition

Information on the composition of juvenile material is available for 28% of the PVs based on macroscopic mineral recognition and/or geochemical analyses. PVs with geochemical analysis account for 23%. The compositions of juveniles in the inventory exhibit a wide range, spanning from basalt to rhyolite (Fig 4). Mafic (45-52 wt.% SiO_2) and intermediate (52-65 wt.% SiO_2) compositions each represent 12% of the structures and are found in various areas and environments within the TMVB. In contrast, felsic compositions (>65 wt.% SiO_2) account only for 4% of the PVs and are predominantly concentrated in the SOVF. Different juvenile compositions can occur in the same area or volcanic field, for example, Valle de Santiago contains PVs with mafic, intermediate, and felsic compositions. A PV, Joya de Estrada maar, with two types of juveniles (felsic and intermediate) has also been identified there.

Alkali data (K_2O and Na_2O) is available for 18% of the PVs. Of these, 12% are calc-alkaline and occur in several areas of the TMVB, as expected in a subduction-related volcanic arc. However, Valle de Santiago contains alkaline (6%) as well as calc-alkaline PVs.

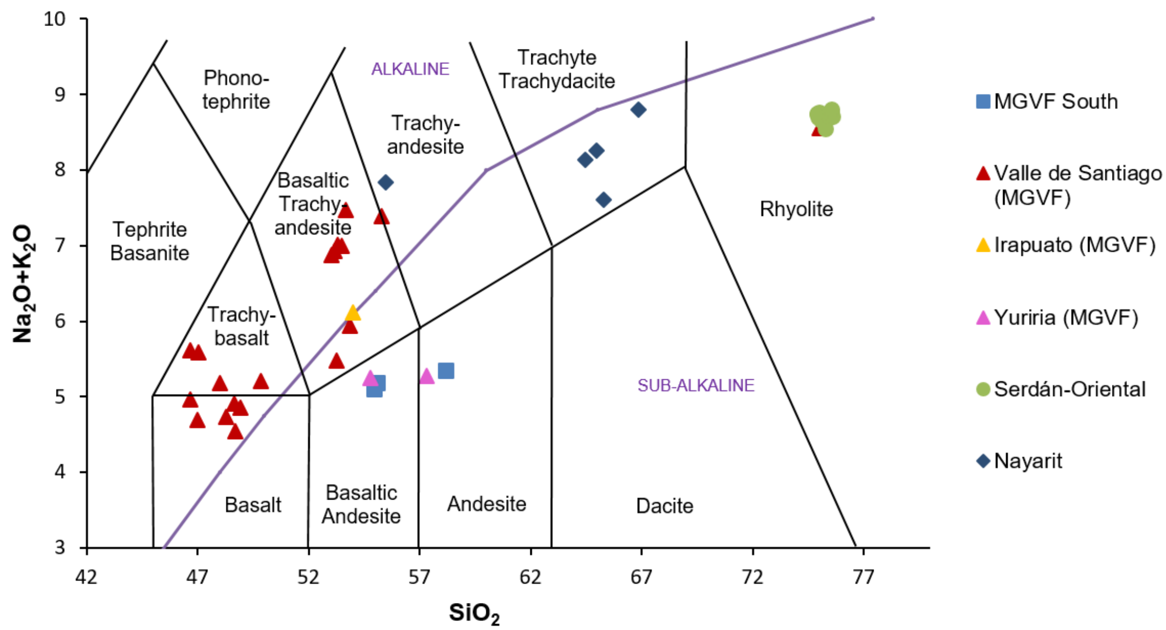

Fig 5. TAS diagram in which 40 analyses of juvenile samples from 16 PVs in 6 areas in the inventory are plotted.

3.5. Ages

Age data is available for 28% of the inventory based on different dating techniques (e.g., radiocarbon dating of paleosols and crater lake sediments, Ar-Ar, and K-Ar; Supplementary file B) which have helped to establish that most of the dated structures formed in the Late Pleistocene (17%) and Holocene (10%) (Fig 6**¡Error! No se encuentra el origen de la referencia.**). Around 18% of PVs have been dated by applying the radiocarbon method to paleosols with maximum ages ranging between ~32,000 and ~1600 yr. BP.

In the LTVF are only two PVs with radiocarbon Holocene age information (e.g. Laguna de Nixtamalapan and Laguna de Apompal, Nelson and González-Caver, 1992). Most of the PVs in the LTVF are classified as not preserved due to syn- or post-volcanic activity, erosion or anthropic activity. However, it has been inferred that the monogenetic volcanoes within this field are Late Pleistocene (<50,000 yr) to Holocene in age (Nelson and González-Caver, 1992; Sieron et al., 2021; Rodríguez-Elizarrarás et al., 2023).

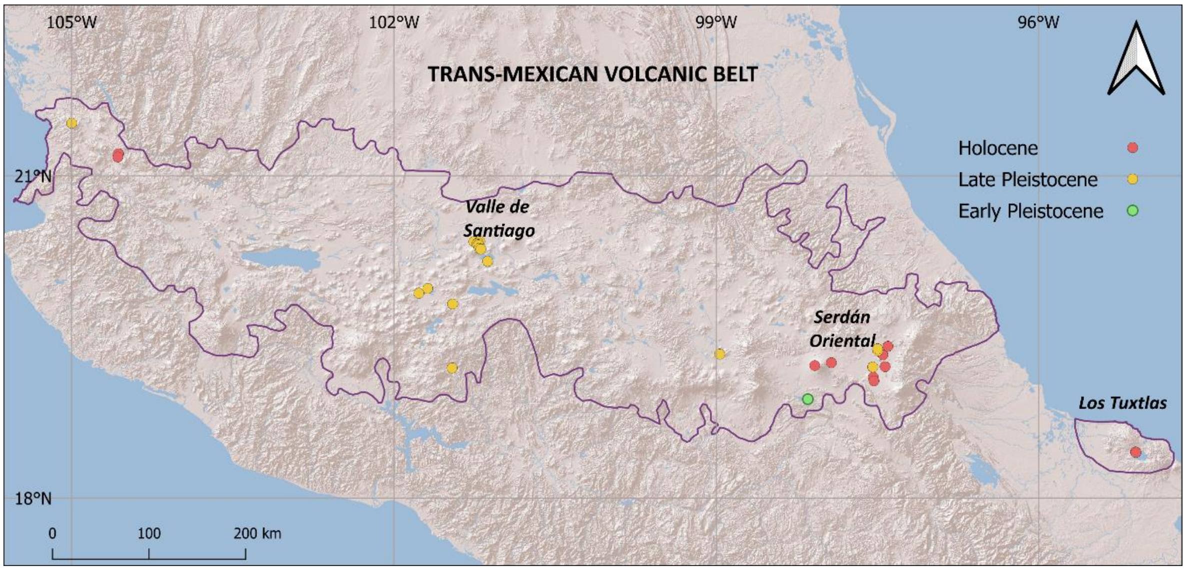

Fig 6. Map showing the location and distribution of dated PVs in the TMVB.

3.6. Morphometry

The morphometric parameters related to the size of the structures, including height (Hco), crater diameter (Wcr), and cone diameter (Wco), exhibit a high CV exceeding 0.3 (Table 3), which indicates a high variability of the values. The TC structures generally have a lower CV compared to the MD-TR structures. Moreover, within both types of structures, the CV as well as the range in the preserved groups tend to show a lower dispersion, with a few exceptions. Detailed statistical descriptors can be accessed in Supplementary File C.

Table 3. Summary of the statistical descriptors of the morphometric parameters and ratios of the PVs in the inventory (Inv) with the data of the preserved sub-set (Pre). N = number of PVs analyzed, Min = minimum value, Max = maximum value, Hco = cone height, Wcr = crater diameter, Wco = cone diameter, A = crater area, AR = aspect ratio, E = elongation, IC = isoperimetric circularity.

Parameters		Type of Structures			
		MD-TR		TF	
		Inv	Pre	Inv	Pre
Hco (m)	N	78	13	19	7
	Median	25.69	30.50	67.00	63.63
	CV	0.86	0.82	0.54	0.38
Wcr (m)	N	63	13	15	7
	Median	1069.50	1095.00	790	737.50
	CV	0.50	0.45	0.34	0.33
Wco (m)	N	41	11	15	7
	Median	1771.50	1771.50	1407.50	1325.00
	CV	0.47	0.43	0.30	0.34
Hco/Wcr	N	60	13	15	7
	Median	0.03	0.04	0.09	0.09
	CV	0.61	0.47	0.97	0.49
Hco/Wco	N	37	11	15	7
	Median	0.02	0.02	0.05	0.05
	CV	0.55	0.45	0.47	0.28
Wcr/Wco	N	39	11	13	7
	Median	0.64	0.63	0.54	0.61
	CV	0.15	0.14	0.28	0.24
AR	N	63	13	15	7
	Median	0.85	0.85	0.74	0.70
	CV	0.14	0.05	0.17	0.09
EL	N	38	13	11	7
	Median	0.82	0.82	0.64	0.62
	CV	0.14	0.08	0.18	0.18
IC	N	38	13	11	7
	Median	0.96	0.97	0.93	0.93
	CV	0.04	0.03	0.05	0.03

3.6.1. Size of maar-diatremes and tuff rings (MD-TR)

The MD-TR main group presents minimum and maximum values between 1 m and 153 m for Hco, from 221 m to 3405 m for Wcr, and between 957 m and 5145 m for Wco. Their respective median values are 26 m, 1070 m, and 1772 m. The median values of the preserved structures are slightly higher for Hco and Wcr, while for Wco the values remained the same as the main group.

MD-TRs formed in MVS, not related to composite volcanoes, present bigger dimensions, with a significantly bigger median Wcr of 1245 m, compared to the MVFs associated with composite volcanoes (e.g., Los Tuxtlas) whose median Wcr is 784 m. Valle de Santiago shows larger median values compared with the other clusters and the scattered group, with a Hco of 38 m, Wcr of 1545 m, and Wco of 2681 m. The median Hco is higher for structures formed in a fluvial environment with

27 m, but MD-TRs in lacustrine environment are much wider with median Wcr of 1228 m and Wco of 1806 m.

The sub sets analyzed for composition and age are small groups of 7 to 11 structures. Mafic MD-TRs tend to be higher (median Hco=40 m) and with wider craters (median Wcr = 1408 m) compared to the structures of intermediate composition. Regarding the age, Late Pleistocene MD-TRs are higher (median Hco = 35 m) but Holocene structures have wider craters (median Wcr = 1245 m).

3.6.2. Size of tuff cones (TCs)

The TC main group presents minimum and maximum values between 20 m and 212 m for Hco, from 342 m to 1140 m for Wcr, and from 555 m to 2098 m for Wco. The median values of these parameters are 67 m, 790 m and 1408 m, respectively. The sub-set of the preserved TCs has lower median values compared to the main group. The majority of the TCs are scattered or isolated, with a few exceptions that occur with clustered MD-TRs, and more often in MVFs (Fig 7), with morphometric parameters median values similar to the main group trend. TCs in fluvial environments and within exorheic basins display higher values for Hco, Wcr and Wco compared to other hydrological environments.

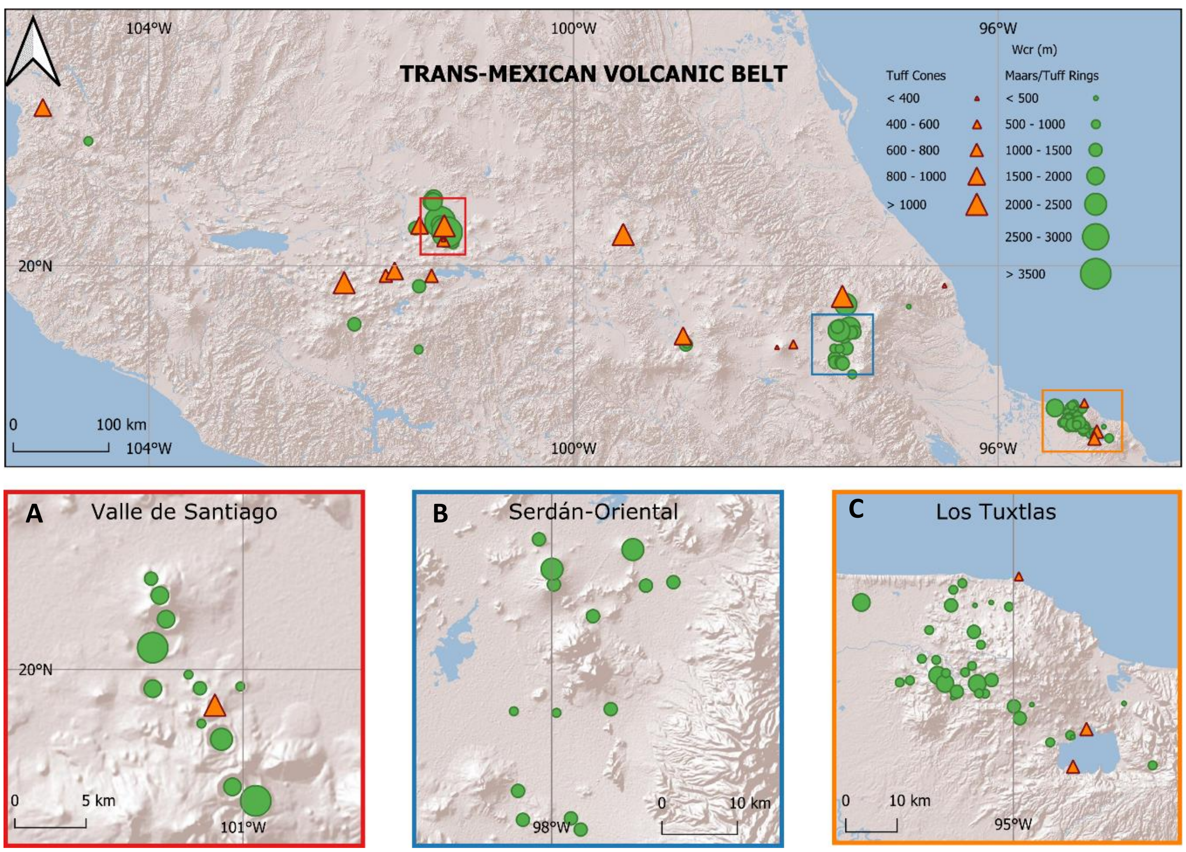

Fig 7. Spatial distribution of PVs within the TMVB showing the variation of their Wcr. Inset maps A, B, C show areas with high concentration of PVs (≥14). A) Valle de Santiago, B) Serdán-Oriental, and C) Los Tuxtlas.

3.6.3. Morphometric ratios

Morphometric ratios for the main group of MD-TRs range from 0.01 to 0.1 for Hco/Wcr and for TCs varies between 0.05 and 0.57. Hco/Wco range from 0.01 to 0.04 for MD-TRs and from 0.03 to 0.013 for TCs. The values of Wcr/Wco range from 0.43 to 0.89 for MD-TRs and from 0.23 to 0.77 for TCs. Corresponding median values are 0.03, 0.02, and 0.64 for MD-TRs, while for TCs they are 0.09, 0.05, and 0.54.

The ranges covered for the preserved sub-sets of structures are less dispersed (Fig 8), and median values, reported in Table 4, are similar to the main group trends, except for Hco/Wco and Wcr/Wco of the preserved TCs which are notably lower compared to the main group. In general, morphometric values of the PVs in this inventory are consistent with reports of structures from other parts of the world (Table 4). This research provides one of the few reports of Hco/Wcr ratio for TCs.

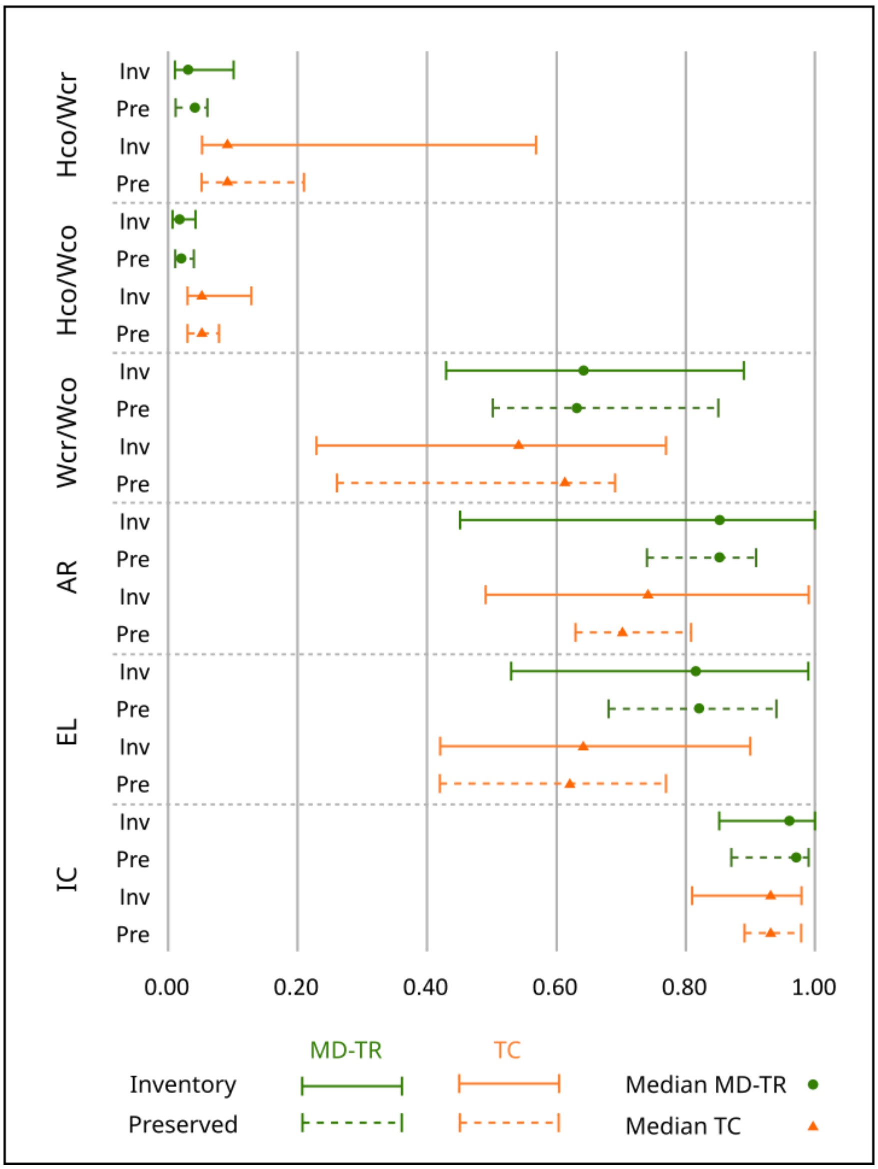

Fig 8. Ranges of the different morphometric ratios of the main groups of MD-TR and TCs in the TMVB and their preserved sub sets. Inv: Full inventory, Pre: Preserved structures.

*Table 4. Morphometric parameters ratios of phreatomagmatic volcanoes reported in previous studies from other regions in the world. Values reported from this research correspond to the group of preserved PVs in the TMVB. *Median values (this research).*

Volcano	**Type**	**Hco (m)**	**Wco (m)**	**Wcr (m)**	**Hco/Wco**	**Hco/Wcr**	**Wcr/Wco**	**AR**	**EL**	**IC**	**Reference**
Tuff cones											
La Caldera de Montana	tuff cone	109	1555	1106	0.07	0.1	0.71				Kervyn et al (2012);
MVs at Deception Island, Antarctica	tuff cones	20.5 - 84.5	310 - 1634	230 - 894	0.04 - 0.16		0.42 -0.74	0.71 - 0.95	0.65 - 0.96	0.83 - 0.99	Pedrazzi et al. (2020)
Trans-Mexican Volcanic Belt (TMVB)	*tuff cones*	*35 - 110 (64)**	*555 – 1990 (1325)**	*342 - 1140 (738)**	*0.03 - 0.08 (0.05)**	*0.05 - 0.21 (0.09)**	*0.26 - 0.69 (0.61)*	*0.63 - 0.81 (0.70)**	*0.42 - 0.77 (0.62)**	*0.89 - 0.98 (0.93)*	*This research*
Maar-diatremes and Tuff rings											
74 maars in different parts of the world	maar-diatremes	4 - 167	91 - 8750	31 - 4000	0.004 - 0.1	0.01-0.17	0.34 - 0.82				Pike (1978)
Crater Elegante, Mexico	tuff ring	50	3350	1600	0.01	0.03	0.48				Wohletz and Sheridan (1983)
Kilbourne Hole, New Mexico	tuff ring	50	5600	2500	0.01	0.02	0.45				Wohletz and Sheridan (1983)
MaarVLS	maar-diatremes			69-5000				0.8 - 0.95	0.84 - 0.88	0.9 - 1	Graettinger et al. (2018)
MVs at Deception Island, Antarctica	tuff ring	5.5 - 95	543 -2323	342 - 1379	0.01 - 0.04		0.52 - 0.67	0.59 - 0.97	0.54 - 1	0.97 - 0.98	Pedrazzi et al. (2020)
Trans-Mexican Volcanic Belt (TMVB)	*maar-diatremes and tuff rings*	*8 - 124 (31)**	*1286- 4559 (1772)**	*336 - 2265 (1095)**	*0.01 - 0.04 (0.02)**	*0.01 - 0.06 (0.04)**	*0.5 - 0.85 (0.63)**	*0.74 - 91 (0.85)**	*0.68 - 0.94 (0.82)**	*0.87 – 0.99 (0.97)**	*This research*

3.6.4. Shape

The shapes of the craters of the PVs within the inventory have been classified into 3 categories: circular, compound, and elongated (Fig 9). *Compound* refers to irregular shapes formed by the overlapping of explosion sites during the phreatomagmatic eruption. *Elongated* refers to elliptical geometries of a crater. Additionally, quantitative shape ratios AR, EL, and IC were calculated for those structures with enough information regarding the measurements of crater diameters, areas, and perimeters.

Structures with elongated craters represent 35% of the inventory, displayed in 30% of the MD-TR and 55% of the TC groups. The predominance of the elongated crater shape is also reflected in the AR and EL median values of 0.85 and 0.82 for MD-TRs and 0.74 and 0.64, respectively, for TCs. Circular crater shapes represent 25% of the inventory, 25% of MD-TRs, and 20% of TCs. Elongated crater shapes display the largest median values for Hco, Wcr, and Wco, while circular PVs display the smallest values. Compound crater shapes represent 15% of the inventory with a similar percentage in each group of structures. The curvature variation in the crater shapes is not significant, indicated by IC median values of 0.96 and 0.93 for MD-TR and TC main groups, respectively.

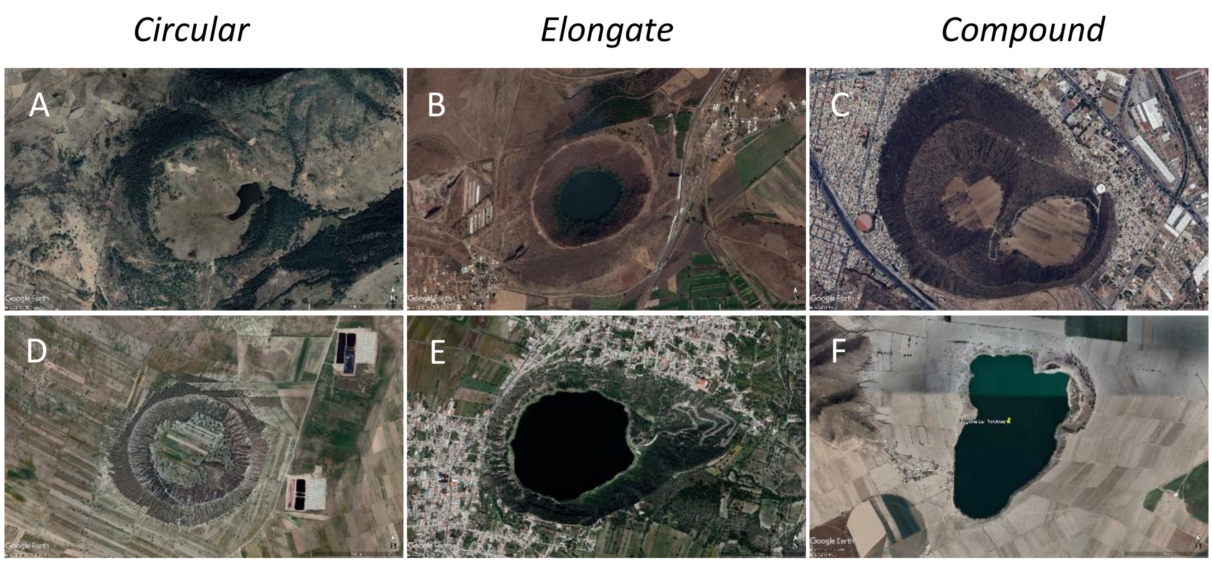

Fig 9. Examples for circular, elongate and compound shapes of tuff cones (TC group). A) Las Vívoras, B) Alberca de Los Espinos, and C) La Caldera; and for maar-diatremes and tuff rings (MD-TR group); D) Tepexitl, E) Laguna Aljojuca, and F) Laguna La Preciosa.

4. Discussion

The inventory of PVs within the extensive area of the TMVB enables closer observations of diverse environments. These areas showcase successful formations of phreatomagmatic structures resulting from the combination of internal and external factors.

4.1. Morphometric correlations

Ratios derived from morphometric parameters have served the purpose of characterizing and distinguishing various types of volcanic structures. Among the commonly employed ratios are

Hco/Wco, Hco/Wcr, and Wcr/Wco (Porter, 1972; Wood, 1980). These ratios were initially proposed to describe deviations from an ideal scoria cone, but as morphological research progressed, ranges of these values were also determined for phreatomagmatic structures (Table 4). Moreover, correlations between morphometric parameters have proven instrumental in distinguishing tuff

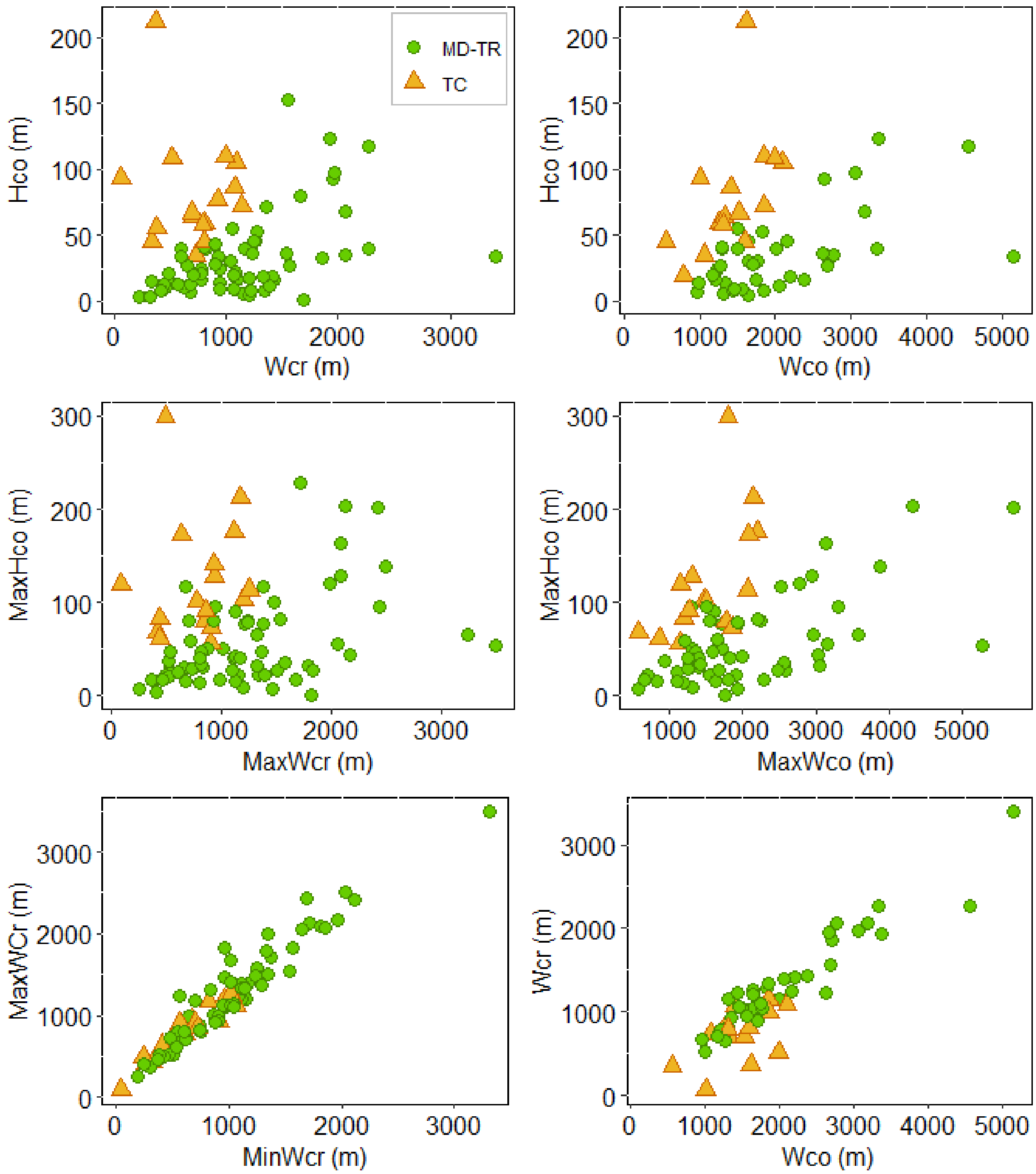

Fig 10. Correlation plots between morphometric parameters Hco, MaxHco, Wc, MaxWc, Wco, and MaxWco.

rings from tuff cones (Pedrazzi et al., 2020).

In correlation scatterplots, morphometric parameters such as Hco, Wcr, Wco, and their maximum values exhibit two overlapping areas within the TC and MD-TR sub-sets (Fig 10). Notably, MD-TRs tend to encompass wider ranges of values, while TCs demonstrate a more restricted range. This overlap could stem from various causes. One could be the variability in eruptive styles, distinguishing between magmatic and phreatomagmatic phases. This variability influences the construction process of volcanic structures, resulting in a diverse array of shapes, reflected in the diffuse trends observed between these types of PVs. Structures with morphometric ratio values inconsistent within the group (TC or MD-TR) are more common in cases of poorly preserved PVs where the tephra ring was affected by syn- and post-eruption processes (e.g., lava flow or scoria cone formation) as well as by the influence of the pre-existing topography (e.g., El Caracol tuff cone, Hco/Wcr = 0.12).

Another factor contributing to the overlap may relate to the accuracy of elevation data, which given the characteristics of Google Earth Pro, proves sometimes challenging to assess. Nevertheless, despite limitations in vertical scale accuracy, the morphometric data still enables clear distinctions within both primary groups of PVs. While it might be possible to reclassify some PVs, especially those within the overlapping area, further in-depth research into specific characteristics of these structures would be necessary to warrant such changes in classification.

The morphometric values Hco and Wcr observed in Valle de Santiago stand out notably, consistently ranking among the highest in their respective categories (Hco = 38 m, Wcr = 1545 m, Wco = 2681). In contrast, Serdán-Oriental, which boasts a higher number of preserved and younger structures (from a similar total analyzed), often showcases lower values in morphometric parameters (Hco = 16m, Wcr = 1234 m, Wco = 1947 m). This discrepancy prompts an exploration into the specific conditions in Valle de Santiago that favor such robust formation of PVs. Both Valle de Santiago and Serdán-Oriental are MVFs, but differences in their hydrogeological environment could be causing the contrasting morphology, as proposed by Lorenz (2003) especially with regard to the Hco of PVs. Valle de Santiago occurs in a fluvial hydrological context within an exorheic basin. It is surrounded by several small-to-medium sized shield volcanoes and small scoria cones, along with lava flows, all set within an aquifer environment dominated by fractured hard-rock in its altitudinal lower area. Conversely, Serdán-Oriental is a lacustrine setting within an endorheic basin surrounded by important stratovolcanoes, including La Malinche and Pico de Orizaba. The PVs in this volcanic field predominantly reside on a soft-rock aquifer host. Despite these differences, there is no discernable pattern between environmental parameters and morphometric values.

The clustered occurrence of PVs in the TMVB suggests that local conditions in specific areas facilitate successful PV formation with sustained water-magma interaction. However, while the types of structures show distinct groupings when morphometric parameters are correlated, environmental parameters (e.g., hydrological environment, type of aquifer host) do not show any correlation with these features (Supplementary files D and E). An interesting observation emerges from the scattered group of MD-TRs (14), revealing consistently moderate to low coefficient of variation (CV) values (ranging from 0.34 to 0.55) in parameters such as Wcr, Hco, and MaxHeight. This trend suggests a relatively uniform nature within this sub-set, contrasting with clustered sub-sets like Valle de Santiago (14), which exhibit higher to moderate CV values (ranging from 0.49 to 0.83). These finding appears counterintuitive since one might expect the scattered sub-set to reflect a broader range of environmental conditions, thereby indicating higher variability. Taking these various observations into account we conclude that environmental parameters and their various combinations could facilitate the conditions for a successful water-magma interaction, however their influence during the building processes of PVs is possibly limited in comparison to the internal eruptive parameters.

4.2. Influence of internal parameters

Changes in eruptive style and a shift of the vent location are common and both influence directly the shape of PVs and the type of monogenetic volcanoes formed (Ort and Carrasco-Núñez, 2009; Kshirsagar et al., 2016; Agustín-Flores et al., 2021). For example, near Catemaco Lake in the LTVF, scoria cones and phreatomagmatic structures formed during the same eruption, accompanied by a shifting of the vent location (e.g., Lagunas de Nixtamalapan and Amolapan in LTVF, Nelson and González-Caver, 1992). Within our inventory at least 20 PVs presumably formed with an initial, late, or intermittent magmatic phase. Elongated and compound shapes (~50% of the inventory) could indicate that a shift of the explosion location occurred, as suggested by Graettinger and Bearden (2021).

Several cases have been reported in which, despite the presence of an aquifer, water-magma interaction during an eruption occurred only until the magmatic flux conditions allowed it (e.g., Miyakejima Volcano, Gutmann, 2002; Geshi et al., 2019). This suggests that the internal parameters exert an important control in the formation of PVs, especially the magma flux and its stability during the eruption.

4.3. Influence of faulting and stress regimes

Stress regime and pre-existing faulting is considered an influencing factor in the crater shape of the structures, the distribution of monogenetic structures (Nakamura et al., 1977; Cebriá et al., 2011; Le Corvec et al., 2013), and also in the hydrogeological dynamic of fracture-controlled aquifers (Lorenz, 2003). However, literature review and observations of the inventory data lead us to conclude that for PVs in the TMVB this influence is not usually significant in the mentioned aspects.

Along the TMVB, monogenetic volcanic alignments have been associated with regional extensional stress regimes and their related fault systems (Demant, 1978; Suter et al., 2001; Urrutia-Fucugauchi and González-Morán, 2006; Sieron et al., 2021). In the Valle de Santiago area, the distribution of PVs does not follow the regional E-W to ENE-WSW trend as do the other neighboring volcanic structures. Instead, PVs show a NNW-SSE oriented, narrowly-aligned distribution, which along with geochemical analyses has been interpreted as evidence for a tear in the subducting Cocos plate (Losantos et al., 2017). According to Uribe-Cifuentes and Urrutia-Fucugauchi (1999) this is a fault zone that has facilitated the rise of magma and also controlled the groundwater flow, providing the conditions for water-magma interaction. However, other important younger regional active fault systems exist, with clear morphological expressions in the terrain, and seem to have influenced the ENE-WSW distribution of scoria cones and shields in the northern part of the MGVF (Hasenaka and Carmichael, 1985; Gómez-Vasconcelos et al., 2020). Moreover, current hydrogeological models based on hydraulic measurements in local wells have determined that the groundwater flows toward the central area of the basin (Lesser y Asociados, 2000; CONAGUA, 2020a) and away from the aligned cluster of PVs, an observation that does not support the notion of a fracture-controlled aquifer.

In Serdán-Oriental the PVs are distributed in an NNE-SSW oriented stripe. Within this stripe, alignments of scoria cones, domes, and PVs occur either in an E-W (Ort and Carrasco-Núñez, 2009;

De León-Barragán et al., 2020) or a NW-SE direction (Guilbaud et al., 2022). These alignments have been interpreted to originate from a structural control on the final ascent of magmas, although morphological evidence of faulting in this area is not obvious.

In the LTVF, the tectonic regime is dominated by lateral slip causing trans-pression and trans-tension in a NW-SE direction (Andreani et al., 2008). Volcanic structures, especially scoria cones, are aligned and cluster along a NW-SE axis that traverses the summit area of the broad San Martín composite volcano (Sieron et al., 2021). However, PVs display a different distribution, occurring mainly on the W and SW lower flanks of San Martín, with fewer on the SE flank.

The shape of PV craters in the inventory (direction of maximum elongation) does not show any preferential direction in either of the mentioned volcanic fields, which leads to the conclusion that the regional stress field does not have a significant influence on the near-surface migration of explosion locations during a phreatomagmatic eruption. This has been also reported for maars in other volcanic fields (Nichols and Graettinger, 2021) and could be explained by local stress variations caused by the explosive eruption itself inducing magma diversion and influencing crater shape (Le Corvec et al., 2018). Another possibility is that in soft-rock hosted aquifers, such as in the Serdán-Oriental, magma can form sills. This would explain a lateral migration of explosion locations that is not controlled by faults during a phreatomagmatic eruption (Nichols and Graettinger, 2021).

4.4. Hydrogeological environments for PVs in the TMVB

4.4.1. Aquifers in lava flows

More than 1400 volcanoes occur within the MGVF. Most of them are shields and scoria cones, as well as cone-less isolated lava flows (Hasenaka, 1994). Shield volcanoes started forming since at least ~2.3 Ma ago (Ban et al., 1992), and scoria cones are usually younger (<1 Ma) than most shields (Hasenaka and Carmichael, 1985; Guilbaud et al., 2012; Avellán et al., 2020). Strombolian eruptions, largely basaltic-andesitic to andesitic in composition, formed these scoria cones and generated significant volumes of lava flows. These flows are often interbedded with fallout and other pyroclastic deposits and display dominantly A'a- and blocky-type morphologies (Hasenaka, 1994; Guilbaud et al., 2011; Avellán et al., 2020).

The anisotropic lithological and hydraulic properties within lava flows or lava flow successions imply that aquifers in this environment display heterogeneous behaviors. Related to this, A'a type lava flow properties locally enhance vertical rainfall recharge, helping to form perched aquifers and providing larger water discharge (Bertrand et al., 2010). Also, lava flows related to scoria cones receive the precipitation captured by the permeable materials that built the cones and that form a thin water table at the base of the structure. It is proposed in this study that highly anisotropic lava flow aquifers may define the hydrogeological conditions, promoting the occurrence of perched aquifers in vast parts of the MGVF. This would explain the scattered distribution of few PVs within large parts of this field, especially in the middle and south.

While in the northern part of the MGVF there are also shield volcanoes, lava flows, and scoria cones, the hydrogeological conditions seem to be different. This area includes the Valle de Santiago field, which holds an important PV cluster (14 structures) within the TMVB. This high frequency of structures within a small area does not match the notion of anisotropic perched lava aquifers that seemingly predominate in most parts of the MGVF. Hydrologically, Valle de Santiago is in an exorheic basin drained by the Río Lerma. The groundwater is hosted in two types of sequences. The upper part consists of granular fluvial and lacustrine deposits interbedded with lava flows, while the lower part is dominated by fractured hard-rock with intercalations of volcaniclastic deposits (Lesser y Asociados, 2000; Mejía-Gómez and Sandoval-Minero, 2004; CONAGUA, 2020a). The combination of porous and fractured media in the lower aquifer could result in an enhanced permeability, with higher vertical hydraulic conductivity, manifested in the high productivity of water wells that reach into deeper parts of the aquifer (Lesser y Asociados, 2000). Currently, information is not sufficient to clearly define the dynamic of the Valle de Santiago aquifer. However, it has been pointed out that the aquifer is broad and highly productive, which we believe is the main reason behind the high frequency of PVs in this area.

On the other hand, large lava flows have the potential to form regional aquifers in the contact zone with an underlying impermeable sedimentary or crystalline substratum (Hunt, 1996; Bertrand et al., 2010). We propose that these are the hydrogeological conditions that influence the formation of the largest PV cluster within the entire TMVB in LTVF (43 structures). The aquifer in the LTVF is characterized by a continuous water table hosted above the contact zone between permeable Upper Miocene lava flows and the underlying Paleogene-Neogene marine clayey sedimentary basement (Nelson and González-Caver, 1992; CONAGUA, 2020b; Rodríguez-Elizarrarás et al., 2023). To the SW of the broad San Martín volcano the water table is shallow (Nelson and González-Caver, 1992) and is where most of LTVF PVs are located.

4.4.2. Lacustrine environments in eastern central Mexico

Serdán-Oriental is an endorheic basin with a combined host aquifer formed by lava flows and volcaniclastic sandy fluvial deposits named Toba Café (Ort and Carrasco-Núñez, 2009; CONAGUA, 2020c). It is likely that the underlying Cretaceous limestone basement overlain by andesites may be hosting a deeper intensely fractured aquifer (Carrasco-Núñez et al., 2007; Guilbaud et al., 2022). Small saline lakes used to form in the central parts of the basin when the water table raised in years of higher precipitation (Ort and Carrasco-Núñez, 2009). In past decades, however, this has no longer happened because of aquifer deterioration due to unfavorable climate effects (e.g., negative balance between annual precipitation and evaporation of -1318 mm/yr) and excessive water extraction for irrigation. Before, all parameters combined (including precipitation) would favor saturation of a regional aquifer in the Serdán-Oriental, which provided the conditions for phreatomagmatic eruptions.

The Sierra Chichinautzin volcanic field forms a topographic high to the south of the endorheic Mexico Basin. The northeastern part of the field extends into the lacustrine basin, where several small-volume monogenetic volcanoes, together with three PVs (La Caldera tuff cone, Xico and Cerro del Marqués tuff rings) occur in the Chalco sub-basin. Conditions do not seem to be sufficient to produce phreatomagmatic eruptions more frequently. Several aligned scoria cones (Sierra de Santa Catarina) show phreatomagmatic deposits at their base (Jaimes-Viera et al., 2018), suggesting that conditions for phreatomagmatism prevailed only briefly during their initial eruptive phases.

Both basins, Serdán-Oriental and the Chalco sub-basin (in the NE part of the Sierra Chichinautzin volcanic field), are apparently similar, however, the frequency of PV formation does not reflect these similarities. It seems that the aquifer in the Mexico basin and its sub-basins (e.g., Chalco) is heterogeneous (CONAGUA, 2020d), suggesting that the ideal regional or continuous character of the aquifer to favor water-magma interaction is not achieved.

Valsequillo is another lacustrine basin in the inventory. It is exorheic and the stratigraphy is formed by a succession of sediments produced by fluvial and lacustrine dynamics interbedded with pyroclastic deposits as well as lava flows. Climate conditions in this basin used to be more humid than at present, and there is evidence that there were lacustrine conditions before the formation of the Toluquilla tuff cone in the Early Pleistocene, 1.30 ± 0.03 Ma (Feinberg et al., 2009; Metcalfe et al., 2016). This is the only PV reported in this basin, among several other monogenetic volcanos like scoria cones. This information suggests that in this case climate may have played an important temporal influence favoring the conditions that resulted in a predominantly phreatomagmatic eruption, and that those conditions are not met frequently in the area.

4.4.3. Hydraulic and topographic gradients

It has been proposed that the hydraulic gradient, represented by the topographic gradient (Heath, 1983), has a strong influence in creating suitable conditions for a phreatomagmatic eruption (Kshirsagar et al., 2015, 2016). The formation of Alberca de Guadalupe maar was attributed to a higher hydraulic gradient (~0.03) compared to a lower value for El Caracol tuff cone, both located at the margins of the lacustrine Zacapu basin in the northern central part of the MGVF. However, a high hydraulic gradient of ~0.06 was estimated for the area where the San Juanito tuff cone and Potrerillo II tuff ring formed, northwest of Ceboruco volcano in western Mexico. Despite the higher gradient (compared to those of Alberca de Guadalupe and El Caracol) and the inferred high-water table, the eruption of these two PVs turned from an early phreatomagmatic to a magmatic eruptive phase. This change in style was interpreted to reflect a rapid exhaustion of the water supply (Agustín-Flores et al., 2021).

Most PVs in the TMVB are located in valleys draining large shield volcanoes (e.g., San Martín shield volcano in the LTVF), and small-to-medium shields (scutulum) in the MGVF, with a wide range of topographic gradients (Hasenaka, 1994). In some lava aquifers the gradient may play an important role, considering that the water flow is favored longitudinal to the lava flow. However, regional aquifers can develop in lavas with low inclination (Hunt, 1996). All considered, although topographic gradient could have a strong influence in some environments, it does not seem to be a parameter which alone could have a strong control during a phreatomagmatic eruption and is likely surpassed in influence by other factors such as precipitation and hydraulic transmissivity.

4.5. Tuff cones (TCs) environments

The formation of tuff cones generally requires great amounts of shallow standing water (Wohletz and Sheridan, 1983; Lorenz, 2003). Considering this, it is not surprising that around half of the TCs in the inventory are located in close proximity or within inter-montane shallow lake environments like Alberca de Los Espinos and El Caracol in the Zacapu basin, and La Caldera in the Chalco basin. Another example is the La Malinche alluvial fan directed towards the lacustrine Serdán-Oriental basin, where Xalapaxco de Huamantla is located (Abrams and Siebe, 1994).

Unusual environments where TCs have formed are the topographically higher middle slopes of stratovolcanoes. This is the case of La Noria at San Juan and Atitlán at La Malinche stratovolcanos, respectively. Since PVs generally form in low topographic areas, the existence of PVs in this unique environment raises questions regarding the conditions that favored their formation, especially given that they are TCs. Given that the La Noria and Atitlán TCs seem to be formed on top of older permeable pumice deposits (Luhr, 2000; Castro-Govea and Siebe, 2007), the conditions for their formation are comparable to the small volcanic field formed at the Miyakejima volcano summit. Here, a local aquifer formed in upper younger permeable volcano deposits, sealed by older weathered deposits, which facilitated the water-magma interaction when magma flux conditions allowed (Geshi et al., 2019).

Resurgent caldera crater rims represent another environment in which few TCs are formed. Las Víboras and Sotoltepec are two TCs formed inside the calderas of Huichapan and Los Humeros, respectively. Both caldera structures are topographic highs and are located in a fluvial-lacustrine environment. However, inside Huichapan crater there is an exorheic basin, while Los Humeros holds an endorheic crater basin.

4.6. Intra-caldera phreatomagmatic structures

Over twenty small-diameter structures were identified near the arcuate fault zones of Los Humeros caldera, inside and outside of its structural rim. The round morphology with low rims of these small structures suggests that they were formed by explosive eruptions. Some of these craters are clustered, particularly those located in the southeastern area within the caldera, while others are scattered around its margin. Their diameters vary from 80 to 485 m, with a median of 157 m.

Intra-caldera structures have been reportedly formed by phreatomagmatic as well as phreatic eruptions, usually during a post-caldera collapse phase, in 1931 at Aniackchak caldera (Nicholson et al., 2011) and in 2012 at Okmok caldera (Larsen et al., 2015; Unema et al., 2016), both in Alaska. In both cases a magmatic control by a drop in the magmatic flux has been suggested. At Pitón de la Fournaise (La Reunión island) two clusters of small-sized structures similar to those at Los Humeros formed during periods of phreatic and phreatomagmatic eruptions (Michon et al., 2013). One proposed explanation is that magma withdrawal in the main conduit due to lateral effusive eruptions allowed the intrusion of groundwater creating conditions necessary for water-magma interaction. Alternatively, another scenario suggests that shallow aquifers formed temporarily after significant precipitation, increasing the likelihood of explosive water-magma interactions (Michon et al., 2013).

The described processes could explain the small-diameter craters at Los Humeros, considering a scenario where interaction took place between low magma flux activity in the caldera system and a shallow aquifer. This set of conditions could be enhanced by climate conditions and precipitation within the endorheic basin dynamic and fractured aquifer (Cedillo-Rodríguez, 2000) of Los Humeros area and may also explain the high frequency of these small craters. A more detailed description of the small craters in Los Humeros and their deposits, including componentry, glass shape, vesicularity, as well as chemical and dating analyses could significantly contribute to a better understanding of the type of process that originated the possibly phreatomagmatic craters in Los Humeros, including the magma flux control of these types of eruptions.

4.7. Age and paleoclimate

Climatic conditions (e.g., precipitation, mean annual temperature) determine the water availability in a region. However, these environmental conditions can vary through time, and hence exert a temporal control on the conditions favoring phreatomagmatism. Considering the climate variability and periods that may have promoted favorable conditions for phreatomagmatic eruptions, one should look at a local scale and only consider detailed paleoclimate records, which are not always available. Applying adequate techniques for PV dating is crucial. The revision of the ages obtained for several PVs showed that Ar-Ar or K-Ar dating is not suitable for young structures, resulting in the need to date them again by the radiocarbon method (e.g., Sieron and Siebe, 2008; Chédeville et al., 2020).

A possible correlation between important global climate events, such as the Last Glacial Maximum (LGM; 19,000–26,500 Cal BP, Clark *et al.*, 2009), and the prevalence of phreatomagmatic versus magmatic eruptions has been proposed previously (Siebe, 1986; Kshirsagar et al., 2015). However, the LGM is diachronous rather than synchronous in the terrestrial paleoclimate record (Hughes and Gibbard, 2015). The LGM in Mexico has been shown to shift to a period from 20,000 to 14,000 yr BP (Vázquez-Selem and Heine, 2011; Caballero et al., 2022), while other authors claim that a full glacier settled from 27,000 to 14,000 BP (Lozano-García et al., 2015; Holmes et al., 2016). Moreover, short-term climatic oscillations of abrupt warming and cooling within millennial to centennial long periods, as well as seasonal precipitation changes promote high climate variability. This is evident in Late Quaternary local paleoclimate records from studies of sediments in intermontane lake basins and crater lakes (maars) along the TMVB (Correa-Metrio et al., 2012; Lozano-García et al., 2015; Holmes et al., 2016; Alcocer, 2022). Also, orogenic effects observable in different areas within the TMVB (e,g., Serdán-Oriental, MGVF, Mexico Valley) need to be taken into account when trying to correlate climate conditions with phreatomagmatic eruptions frequency (Correa-Metrio et al., 2012; Alcocer, 2022).

Paleosol samples located directly below the deposits of 19 PVs provided 42 radiocarbon analyses, which represent maximum ages of their respective phreatomagmatic eruptions (Supplementary file B). Calibrated BP ages span from the Late Pleistocene (~40,000 yr Cal BP) until recent (1350 yr Cal BP). Formation of PVs took place in humid as well as dry climate condition periods over the past ~50,000 yr Cal BP (Fig 11). In the MGVF, PV formation spans between 40,000 and 11,000 yr BP, including the LGM. In Serdán-Oriental a couple of the structures formed at the beginning of the LGM, but most of the PVs are of Holocene age. The youngest dated PVs are located in Nayarit (e.g., Potrerillo II in Ceboruco Valley) and LTVF (e.g, Laguna Nixtamalapan and Amolapan). More than 40 PVs in the LTVF are Late Pleistocene and Holocene in age, <50,000 yr BP (Nelson and González-Caver, 1992; Sieron et al., 2021; Rodríguez-Elizarrarás et al., 2023). Most of them are quite eroded, which could be attributed to humid climate conditions, since this area has one of the highest current annual precipitation rates in the TMVB (~2900 mm/yr, CONAGUA).

Despite periods of stable climate conditions, millennial and seasonal variations introduce a significant uncertainty in the assignment of past environment conditions during PV formation. Therefore, although climate may have a temporal control over the conditions for phreatomagmatism, PV formation is likely more related to local variability than global climate events.

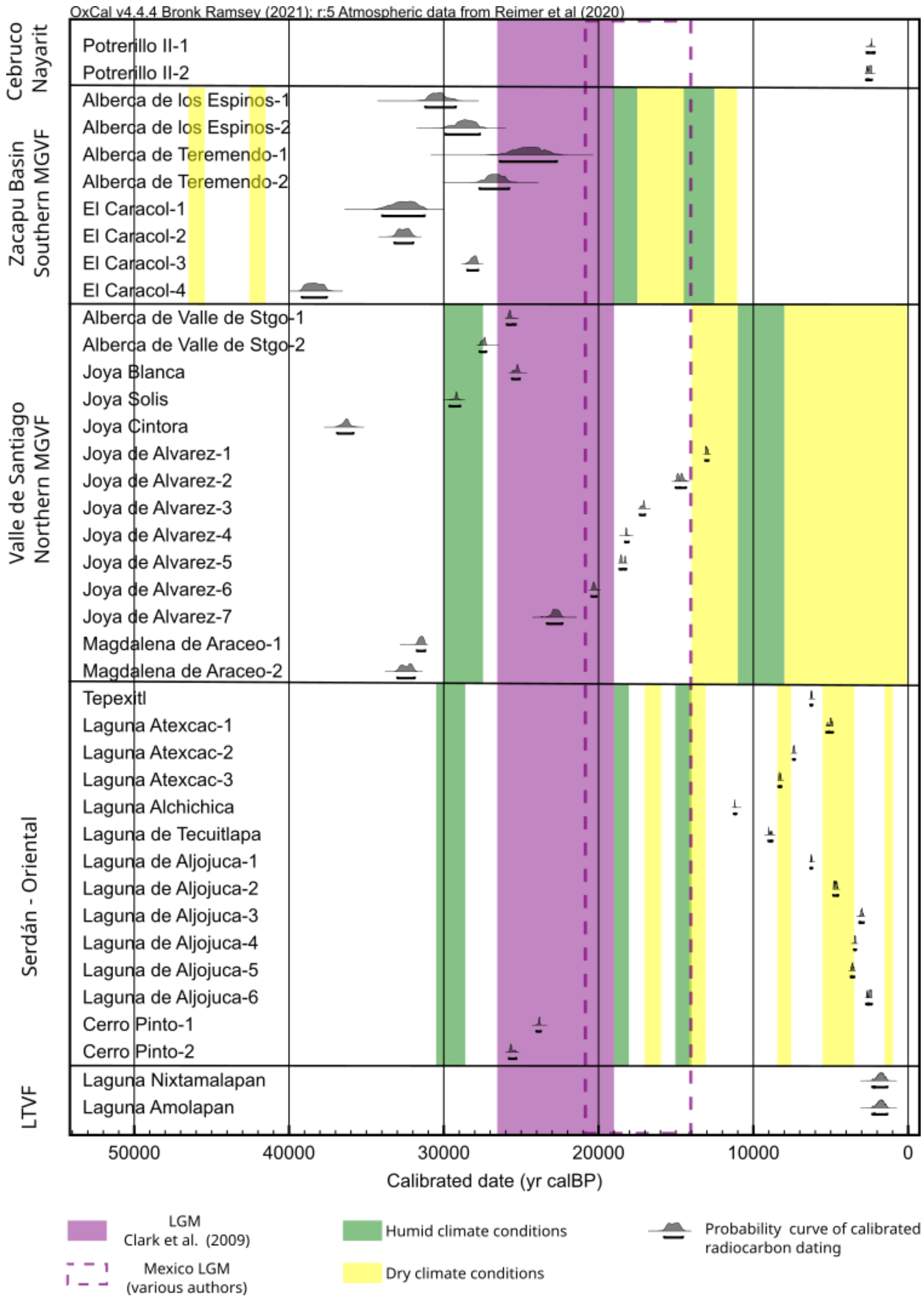

Fig 11. Comparison of calibrated radiocarbon ages (yr Cal BP) of PVs vs. reported climate conditions. Ages calibrated with Oxcal, IntCal20 (Reimer et al., 2020). Dominantly dry and humid periods reported in Correa-Metrio et al. (2012); Lozano-García et al. (2015); Holmes et al. (2016); Caballero et al. (2022).

4.8. Degree of influence of the different parameters

The analysis of the inventory of PVs within the TMVB does not show a simple direct relationship between frequency or type of phreatomagmatic structure and the identified internal and environmental parameters. However, this analysis, together with the information provided by research of phreatomagmatism elsewhere, provided interesting observations regarding the degree of influence of the several parameters involved in a phreatomagmatic eruption.

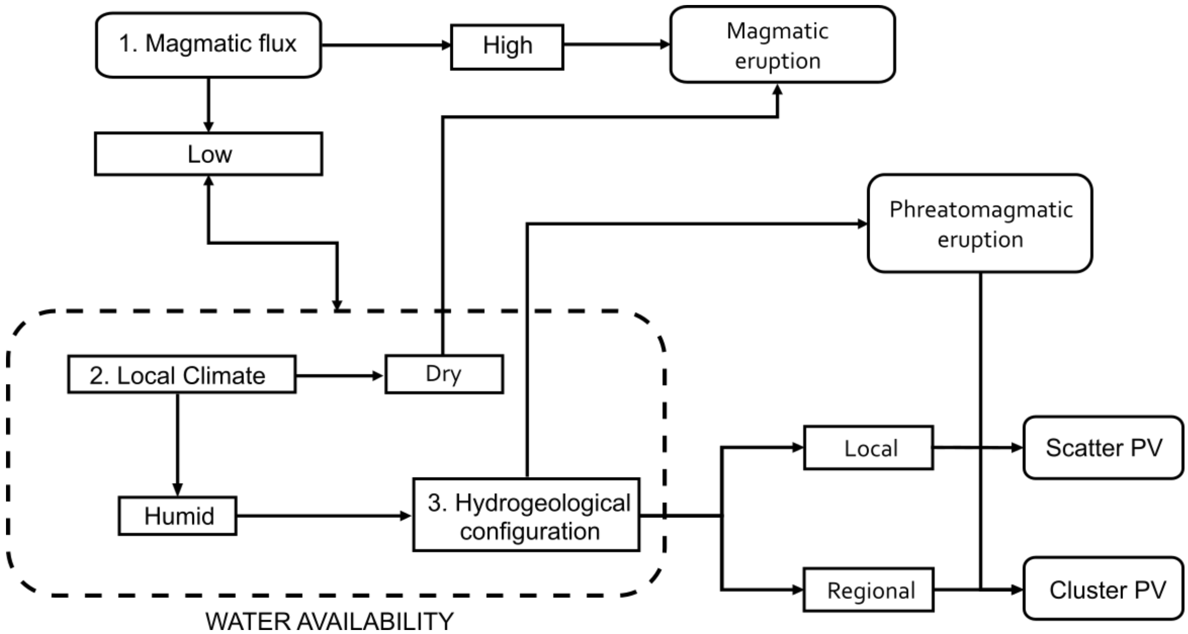

Fig 12. Flow diagram of the influence and interaction between the main parameters involved in water-magma interaction. A first-degree influence is the magmatic flux, followed by the parameters that control water availability with climate as second-degree and hydrogeological conditions as a third-degree influence.

We propose that the magmatic flux during an eruption as a first-degree influencing parameter, which can control eruption style and type of resulting monogenetic volcano. Water availability is controlled by the interplay between local hydrogeological conditions and climate. The degree of influence of both varies depending on the location (altitude) of the area. We propose that climate has a second-degree while hydrogeological conditions have a third-degree influence. High-conductivity host aquifers, such as anisotropic lava flows or granular sequences, with humid climates favor productive aquifers. These conditions are enhanced when an aquifer of regional distribution is developed in an active volcanic zone, like the contact zone between lava flows and underlying less permeable material (e.g., LTVF) or the intercalation of granular and fractured aquifer hosts (e.g., Serdán-Oriental and Valle de Santiago fields), resulting in more frequent phreatomagmatic eruptions.

4.9. Research limitations

In this study more than 100 PVs within the TMVB were analyzed. Geological, environmental, and morphometric information was compiled to determine the local conditions where phreatomagmatic structures have successfully formed. The majority of data in this study was acquired from available published documents and government institution public databases. Therefore, data was generated by diverse methodologies and interpreted according to different criteria. Morphometric data precision is determined by the accuracy of the Google Earth Pro geospatial data, especially in terms of the vertical scale.

CONAGUA 2020 reports were the main source of hydrogeological information for this study. However, for the majority of the sites within this inventory there is a lack of information regarding hydrological conditions, and available information typically consists of estimated average or range values for entire aquifers. Considering that most of the PVs tend to be clustered in very specific sites, the conditions of these sites are very localized, hence, regional or average information does not have the ideal resolution for analyzing the conditions that facilitated the formation of phreatomagmatic structures.

In the LTVF it was not possible to measure the morphometric parameters of most of the structures due to their poor preservation. This explains the high variability observed in the different sub-sets where morphometric parameters were analyzed. It would be desirable to obtain more field information and measurements from high-resolution images to remedy this lack of data in one of the main PV clusters in the TMVB.

4.10. PVs possibly not included in the inventory

It is likely that several PVs remain unidentified, especially in large volcanic fields like the MGVF, SOVF, and LTVF. Also, some structures reported before as being phreatomagmatic in origin (e.g., Tío Cheve Maar in XVF, Jácome-Paz et al., 2022) were not included in this inventory due to the lack of convincing evidence observed during field visits. In other cases, both types of fragmentation (magmatic and phreatomagmatic) are present making it unclear which types of activity dominated during their formation (e.g., Acatlán, XVF).

Small-diameter explosion craters in Los Humeros caldera were not included within the main inventory. Instead, their morphometry was analyzed separately since it is unclear if these craters were formed by phreatic or phreatomagmatic eruptions. This distinction is important because there is not direct water-magma interaction during phreatic activity. Also, most of the structures have a much smaller diameter than the median size of the PVs in the inventory and this could skew the results if analyzed along with the rest of the inventory. Further research is required to clarify the type of eruption that originated these structures and whether they should be classified as phreatomagmatic.

5. Conclusions

In this study we compiled an inventory of PVs in the TMVB, a subduction-related volcanic arc under an extensional tectonic regime. The analysis of the inventory revealed a variety of important insights about the different parameters that promote the occurrence of these structures:

- Not surprisingly, most PVs occur in MVFs (91%) where the small-volume magmatic flux is more likely to meet appropriate environmental conditions to generate a phreatomagmatic eruption.
- Maars and tuff rings (MD-TRs) are the most common phreatomagmatic volcano type in the TMVB (81%) and are typically clustered. In contrast, tuff cones (TCs) are less frequent (19%) and tend to be scattered.
- There is a clear morphometric differentiation between MD-TRs and TCs.
- There is no clear correlation between individual environmental parameters and the frequency and size of PVs.
- PVs occur in a wide variety of combinations of external parameters. The most frequent environmental conditions where PVs occur and often cluster have a fluvial dynamic and

combined aquifer host. However, less frequent combinations of parameters also facilitate phreatomagmatism, as reflected in environments where scattered PVs occur. PVs occur very rarely in topographically higher areas (e.g., La Noria and Atitlan tuff cones, located on the slopes of composite volcanoes).

- Areas where an aquifer presents a regional distribution are more likely to form PV clusters.
- PVs (with available dating information) primarily formed during the Late Pleistocene to Holocene, with the exception of Toluquilla (Early Pleistocene).
- We consider magmatic flux at the moment of the eruption to be the first-degree influence to achieve a successful MFCI followed by climate (precipitation) and local hydrogeological configuration.

Further detailed research (e.g., radiometric dating and hydrogeological studies) of individual PVs is required to better understand the eruptive and local hydrogeological dynamics and to expand the understanding of this type of volcanism. Expanding the inventories of phreatomagmatic volcanoes in different environments around the world allows for the study of the diverse conditions in which this type of volcanism occur, and also provides a base of knowledge to prepare for future eruptions.

Acknowledgements

Field and laboratory costs were defrayed by project DGAPA-UNAM IN104221 (Dirección General de Asuntos del Personal Académico, UNAM) granted to C. Siebe. Mélida Schliz-Antequera benefited from a CONAHCYT (Consejo Nacional de Humanidades, Ciencia y Tecnología) doctoral fellowship awarded from 2020-2023. C. Siebe benefited from a sabbatical stay at the Senckenberg Naturhistorische Sammlungen, Dresden and the kind hospitality of Jan-Michael Lange and Peter Suhr.

REFERENCES

Abrams, M.J., Siebe, C., 1994. Cerro Xalapaxco: An unusual tuff cone with multiple explosion craters, in Central Mexico (Puebla). J. Volcanol. Geotherm. Res. 63, 183–199.

Agustín-Flores, J., Siebe, C., Ferrés, D., Sieron, K., González-Zuccolotto, K., 2021. Monogenetic volcanoes with initial phreatomagmatic phases in the Ceboruco graben, western Mexico: The cases of Potrerillo I, Potrerillo II, and San Juanito. J. Volcanol. Geotherm. Res. 412. https://doi.org/10.1016/j.jvolgeores.2021.107184

Albert, H., Costa, F., Martí, J., 2016. Years to weeks of seismic unrest and magmatic intrusions precede monogenetic eruptions. Geology 44, 211–214. https://doi.org/10.1130/G37239.1

Alcocer, J. (Ed.), 2022. Lake Alchichica limnology: The uniqueness of a tropical maar lake, Lake Alchichica Limnology: The Uniqueness of a Tropical Maar Lake. Springer Nature Switzerland AG. https://doi.org/https://doi.org/10.1007/978-3-030-79096-7_3

Andreani, L., Rangin, C., Martínez-reyes, J., Roy, C.L.E., Aranda-garcía, M., Pichon, X.L.E., Peterson-rodriguez, R., 2008. The Neogene Veracruz fault : evidences for left-lateral slip along the southern Mexico block. Bull. la Société géologique Fr. 195–208.

Auer, A., Martin, U., Németh, K., 2007. The Fekete-hegy (Balaton Highland Hungary) “soft-substrate” and “hard-substrate” maar volcanoes in an aligned volcanic complex - Implications for vent geometry, subsurface stratigraphy and the palaeoenvironmental setting. J. Volcanol.

Geotherm. Res. 159, 225–245. https://doi.org/10.1016/j.jvolgeores.2006.06.008

Austin-Erickson, A., Büttner, R., Dellino, P., Ort, M.H., Zimanowski, B., 2008. Phreatomagmatic explosions of rhyolitic magma: Experimental and field evidence. J. Geophys. Res. Solid Earth 113, 1–12. https://doi.org/10.1029/2008JB005731

Avellán, D.R., Cisneros-Máximo, G., Macías, J.L., Gómez-Vasconcelos, M.G., Layer, P.W., Sosa-Ceballos, G., Robles-Camacho, J., 2020. Eruptive chronology of monogenetic volcanoes northwestern of Morelia – Insights into volcano-tectonic interactions in the central-eastern Michoacán-Guanajuato Volcanic Field, México. J. South Am. Earth Sci. 100, 102554. https://doi.org/10.1016/j.jsames.2020.102554

Avellán, D.R., Macías, J.L., Pardo, N., Scolamacchia, T., Rodriguez, D., 2012. Stratigraphy, geomorphology, geochemistry and hazard implications of the Nejapa Volcanic Field, western Managua, Nicaragua. J. Volcanol. Geotherm. Res. 213–214, 51–71. https://doi.org/10.1016/j.jvolgeores.2011.11.002

Ban, M., Hasenaka, T., Delgado-Granados, H., Takaoka, N., 1992. K-Ar ages of lavas from shield volcanoes in the Michoacan-Guanajuato volcanic field, Mexico. Geofísica Int. 31, 467–473.

Barberi, F., Cioni, R., Rosi, M., Santacroce, R., Sbrana, A., Vecci, R., 1989. Magmatic and phreatomagmatic phases in explosive eruptions of Vesuvius as deduced by grain-size and component analysis of the pyroclastic deposits. J. Volcanol. Geotherm. Res. 38, 287–307.

Bertrand, G., Celle-Jeanton, H., Huneau, F., Loock, S., Renac, C., 2010. Identification of different groundwater flowpaths within volcanic aquifers using natural tracers for the evaluation of the influence of lava flows morphology (Argnat basin, Chaîne des Puys, France). J. Hydrol. 391, 223–234. https://doi.org/10.1016/j.jhydrol.2010.07.021

Branney, M.J., Kokelaar, P., 2002. Pyroclastic Density Currents and the Sedimentation of Ignimbrites. Geol. Soc. Mem.

Bronk Ramsey, C., 2009. Bayesian analysis of radiocarbon dates. Radiocarbon 51, 337–360. https://doi.org/10.2458/azu_uapress_9780816530595-ch039

Büttner, R., Dellino, P., La Volpe, L., Lorenz, V., Zimanowski, B., 2002. Thermohydraulic explosions in phreatomagmatic eruptions as evidenced by the comparison between pyroclasts and products from Molten Fuel Coolant Interaction experiments. J. Geophys. Res. Solid Earth 107, ECV 5-1-ECV 5-14. https://doi.org/10.1029/2001jb000511

Caballero, M., Lozano-García, M. del S., Ortega-Guerrero, B., 2022. Paleoenvironmental Change in Central Mexico During the Last 20,000 Years, in: Lake Aichica Limnology: The Uniqueness of a Tropical Maar Lake. pp. 33–50.

Carn, S.A., 2000. The Lamongan volcanic field, East Java, Indonesia: Physical volcanology, historic activity and hazards. J. Volcanol. Geotherm. Res. 95, 81–108. https://doi.org/10.1016/S0377-0273(99)00114-6

Carrasco-Núñez, G., Hernández, J., De León, L., Dávila, P., Norini, G., Bernal, J.P., Jicha, B., Navarro, M., López-Quiroz, P., 2017. Geologic Map of Los Humeros volcanic complex and geothermal field, easternTrans-Mexican Volcanic Belt. Terra Digit. 1, 1–11. https://doi.org/10.22201/igg.terradigitalis.2017.2.24.78

Carrasco-Núñez, G., Ort, M.H., Romero, C., 2007. Evolution and hydrological conditions of a maar volcano (Atexcac crater, Eastern Mexico). J. Volcanol. Geotherm. Res. 159, 179–197. https://doi.org/10.1016/j.jvolgeores.2006.07.001

Castro-Govea, R., Siebe, C., 2007. Late Pleistocene-Holocene stratigraphy and radiocarbon dating of La Malinche volcano, Central Mexico. J. Volcanol. Geotherm. Res. 162, 20–42. https://doi.org/10.1016/j.jvolgeores.2007.01.002

Cebriá, J.M., Martín-Escorza, C., López-Ruiz, J., Morán-zenteno, D.J., Martiny, B.M., 2011. Numerical recognition of alignments in monogenetic volcanic areas : Examples from the Michoacán-Guanajuato Volcanic Field in Mexico and Calatrava in Spain. J. Volcanol. Geotherm. Res. 201, 73–82. https://doi.org/10.1016/j.jvolgeores.2010.07.016

Cedillo-Rodríguez, F., 2000. Hydrogeologic model of the geothermal reservoir from Los Humeros, Puebla, Mexico. Geotherm. Resour. Counc. Trans. 24, 381–409.

Chédeville, C., Guilbaud, M.-N., Siebe, C., 2020. Stratigraphy and radiocarbon ages of late-Holocene Las Derrumbadas rhyolitic domes and surrounding vents in the Serdán-Oriental basin (Mexico): Implications for archeology, biology, and hazard assessment. Holocene 30, 402–419. https://doi.org/10.1177/0959683619887417

Clark, P.U., Dyke, A.S., Shakun, J.D., Carlson, A.E., Clark, J., Wohlfarth, B., Mitrovica, J.X., Hostetler, S.W., McCabe, A.M., 2009. The Last Glacial Maximum. Science (80-.). 325, 710–714. https://doi.org/10.1126/science.1172873

Cole, P.D., Queiroz, G., Wallenstein, N., Gaspar, J.L., Duncan, A.M., Guest, J.E., 1995. An historic subplinian/phreatomagmatic eruption: the 1630 AD eruption of Furnas volcano , São Miguel , Azores. J. Volcanol. Geotherm. Res. 69, 117–135.

CONAGUA, 2020a. ACTUALIZACIÓN DE LA DISPONIBILIDAD MEDIA ANUAL DE AGUA EN EL ACUÍFERO IRAPUATO-VALLE (1119), ESTADO DE GUANAJUATO.

CONAGUA, 2020b. ACTUALIZACIÓN DE LA DISPONIBILIDAD MEDIA ANUAL DE AGUA EN EL ACUÍFERO SIERRA DE SAN ANDRÉS TUXTLA (3016), ESTADO DE VERACRUZ.

CONAGUA, 2020c. ACTUALIZACIÓN DE LA DISPONIBILIDAD MEDIA ANUAL DE AGUA EN EL ACUÍFERO LIBRES-ORIENTAL (2102), ESTADO DE PUEBLA.

CONAGUA, 2020d. ACTUALIZACIÓN DE LA DISPONIBILIDAD MEDIA ANUAL DE AGUA EN EL ACUÍFERO ZONA METROPOLITANA DE LA CD. DE MÉXICO (0901), CIUDAD DE MÉXICO. Ciudad de México.

Correa-Metrio, A., Lozano-García, S., Xelhuantzi-López, S., Sosa-Nájera, S., Metcalfe, S.E., 2012. Vegetation in western Central Mexico during the last 50 000 years: Modern analogs and climate in the Zacapu Basin. J. Quat. Sci. 27, 509–518. https://doi.org/10.1002/jqs.2540

De León-Barragán, L., Carrasco-Núñez, G., Ort, M.H., 2020. Stratigraphy and evolution of the Holocene Aljojuca Maar volcano (Serdán-Oriental basin, Eastern Trans-Mexican Volcanic Belt), and implications for hazard assessment. J. Volcanol. Geotherm. Res. 392, 106789. https://doi.org/10.1016/j.jvolgeores.2020.106789

De Rita, D., Giordano, G., Esposito, A., Fabbri, M., Rodani, S., 2002. Large volume phreatomagmatic ignimbrites from the Colli Albani volcano (Middle Pleistocene, Italy). J. Volcanol. Geotherm.

Res. 118, 77–98. https://doi.org/10.1016/S0377-0273(02)00251-2

Delcamp, A., van Wyk de Vries, B., Stéphane, P., Kervyn, M., 2014. Endogenous and exogenous growth of the monogenetic Lemptégy volcano, Chaîne des Puys, France. Geosphere 10, 998–1019. https://doi.org/10.1130/GES01007.1

Demant, A., 1978. Características del Eje Neovolcánico Transmexicano y sus problemas de interpretación. Rev. Mex. Ciencias Geológicas 2, 172–187.

Dorison, A., Siebe, C., 2023. Evolution of ancient farming systems and demography in the volcanic highlands of Zacapu: A model drawn from Geoarchaeology and archaeogeography. Anc. Mesoamerica 1–26. https://doi.org/10.1017/s0956536122000013

Feinberg, J.M., Renne, P.R., Arroyo-Cabrales, J., Waters, M.R., Ochoa-Castillo, P., Perez-Campa, M., 2009. Age constraints on alleged “footprints” preserved in the Xalnene Tuff near Puebla, Mexico. Geology 37, 267–270. https://doi.org/10.1130/G24913A.1

Ferrari, L., Orozco-Esquivel, T., Manea, V., Manea, M., 2012. The dynamic history of the Trans-Mexican Volcanic Belt and the Mexico subduction zone. Tectonophysics 522–523, 122–149. https://doi.org/10.1016/j.tecto.2011.09.018

Fisher, R. V., 1977. Erosion by volcanic base-surge density currents: U-shaped channels. Bull. Geol. Soc. Am. 88, 1287–1297. https://doi.org/10.1130/0016-7606(1977)88<1287:EBVBDC>2.0.CO;2

Fisher, R. V., Schmincke, H.U., 1984. Pyroclastic Rocks. https://doi.org/10.1007/978-3-642-74864-6

Geshi, N., Németh, K., Noguchi, R., Oikawa, T., 2019. Shift from magmatic to phreatomagmatic explosions controlled by the lateral evolution of a feeder dike in the Suoana-Kazahaya eruption, Miyakejima Volcano, Japan. Earth Planet. Sci. Lett. 511, 177–189. https://doi.org/10.1016/j.epsl.2019.01.038

Gómez-Vasconcelos, M.G., Macías, J.L., Avellán, D.R., Sosa-Ceballos, G., Garduño-Monroy, V.H., Cisneros-Máximo, G., Layer, P.W., Benowitz, J., López-Loera, H., López, F.M., Perton, M., 2020. The control of preexisting faults on the distribution, morphology, and volume of monogenetic volcanism in the Michoacán-Guanajuato Volcanic Field. GSA Bull. 132, 2455–2474. https://doi.org/10.1130/b35397.1

Graettinger, A.H., 2018. Trends in maar crater size and shape using the global Maar Volcano Location and Shape (MaarVLS) database. J. Volcanol. Geotherm. Res. 357, 1–13. https://doi.org/10.1016/j.jvolgeores.2018.04.002

Graettinger, A.H., Bearden, A.T., 2021. Lateral migration of explosive hazards during maar eruptions constrained from crater shapes. J. Appl. Volcanol. 10, 1–14.

Guilbaud, M.-N., Chédeville, C., Molina-Guadarrama, Á.N., Pineda-Serrano, J.C., Siebe, C., 2022. Volcano-sedimentary processes at Las Derrumbadas rhyolitic twin domes, Serdán-Oriental Basin, Eastern Trans-Mexican Volcanic Belt. Geol. Soc. London, Spec. Publ. 520, 165–189. https://doi.org/https://doi.org/10.1144/SP520-2021-144

Guilbaud, M.N., Siebe, C., Layer, P., Salinas, S., 2012. Reconstruction of the volcanic history of the Tacámbaro-Puruarán area (Michoacán, México) reveals high frequency of Holocene monogenetic eruptions. Bull. Volcanol. 74, 1187–1211. https://doi.org/10.1007/s00445-012-

0594-0

Guilbaud, M.N., Siebe, C., Layer, P., Salinas, S., Castro-Govea, R., Garduño-Monroy, V.H., Le Corvec, N., 2011. Geology, geochronology, and tectonic setting of the Jorullo Volcano region, Michoacán, México. J. Volcanol. Geotherm. Res. 201, 97–112. https://doi.org/10.1016/j.jvolgeores.2010.09.005

Gutmann, J.T., 2002. Strombolian and effusive activity as precursors to phreatomagmatism: Eruptive sequence at maars of the Pinacate volcanic field, Sonora, Mexico. J. Volcanol. Geotherm. Res. 113, 345–356. https://doi.org/10.1016/S0377-0273(01)00265-7

Hasenaka, T., 1994. Size, distribution, and magma output rate for shield volcanoes of the Michoacán-Guanajuato volcanic field, Central Mexico. J. Volcanol. Geotherm. Res. 63, 13–31. https://doi.org/10.1016/0377-0273(94)90016-7

Hasenaka, T., Carmichael, I.S.E., 1985. The cinder cones of Michoacán-Guanajuato, central Mexico: their age, volume and distribution, and magma rate. J. Volcanol. Geotherm. Res. 25, 105–124.

Heath, R.C., 1983. Basic ground-water hydrology, in: Geological Survey Water-Supply Paper; 2220.

Henry, C.D., Aranda-Gomez, J.J., 1992. The real southern Basin and Range: Mid- to late Cenozoic extension in Mexico. Geology 20, 701–704. https://doi.org/10.1130/0091-7613(1992)020<0701:TRSBAR>2.3.CO;2

Holmes, J.A., Metcalfe, S.E., Jones, H.L., Marshall, J.D., 2016. Climatic variability over the last 30 000 years recorded in La Piscina de Yuriria, a Central Mexican crater lake. J. Quat. Sci. 31, 310–324. https://doi.org/10.1002/jqs.2846

Houghton, B.F., Schmincke, H.U., 1989. Rothenberg scoria cone, East Eifel: a complex Strombolian and phreatomagmatic volcano. Bull. Volcanol. 52, 28–48. https://doi.org/10.1007/BF00641385

Houghton, B.F., Wilson, C.J.N., Smith, I.E.M., 1999. Shallow-seated controls on styles of explosive basaltic volcanism: A case study from New Zealand. J. Volcanol. Geotherm. Res. 91, 97–120. https://doi.org/10.1016/S0377-0273(99)00058-X

Hughes, P.D., Gibbard, P.L., 2015. A stratigraphical basis for the Last Glacial Maximum (LGM). Quat. Int. 383, 174–185. https://doi.org/10.1016/j.quaint.2014.06.006

Hunt, C.D.J., 1996. Geohydrology of the Island of Oahu, Hawaii, US Geological Survey Professional Paper. https://doi.org/10.3133/pp1412b

Jácome-Paz, M.P., Torres-Orozco, R., Espinasa-Pereña, R., de la Fuente Rivera, J.R., Sánchez, J.O.R., Delgado-Granados, H., 2022. Review of geology and geomorphology of the Xalapa Monogenetic Volcanic Field, eastern Trans-Mexican Volcanic Belt. J. Volcanol. Geotherm. Res. 432. https://doi.org/10.1016/j.jvolgeores.2022.107689

Jaimes-Viera, M.C., Martin Del Pozzo, A.L., Layer, P.W., Benowitz, J.A., Nieto-Torres, A., 2018. Timing the evolution of a monogenetic volcanic field: Sierra Chichinautzin, Central Mexico. J. Volcanol. Geotherm. Res. 356, 225–242. https://doi.org/10.1016/j.jvolgeores.2018.03.013

Kereszturi, G., Németh, K., 2012. Monogenetic Basaltic Volcanoes: Genetic Classification, Growth, Geomorphology and Degradation. Updat. Volcanol. - New Adv. Underst. Volcan. Syst. 16–17.

https://doi.org/10.5772/51387

Kereszturi, G., Németh, K., Csillag, G., Balogh, K., Kovács, J., 2011. The role of external environmental factors in changing eruption styles of monogenetic volcanoes in a Mio/Pleistocene continental volcanic field in western Hungary. J. Volcanol. Geotherm. Res. 201, 227–240. https://doi.org/10.1016/j.jvolgeores.2010.08.018

Kshirsagar, P., Siebe, C., Guilbaud, M.N., Salinas, S., 2016. Geological and environmental controls on the change of eruptive style (phreatomagmatic to Strombolian-effusive) of Late Pleistocene El Caracol tuff cone and its comparison with adjacent volcanoes around the Zacapu basin (Michoacán, México). J. Volcanol. Geotherm. Res. 318, 114–133. https://doi.org/10.1016/j.jvolgeores.2016.03.015

Kshirsagar, P., Siebe, C., Guilbaud, M.N., Salinas, S., Layer, P.W., 2015. Late Pleistocene Alberca de Guadalupe maar volcano (Zacapu basin, Michoacán): Stratigraphy, tectonic setting, and paleo-hydrogeological environment. J. Volcanol. Geotherm. Res. 304, 214–236. https://doi.org/10.1016/j.jvolgeores.2015.09.003

Larsen, J.F., Neal, C.A., Schaefer, J.R., Kaufman, A.M., Lu, Z., 2015. The 2008 phreatomagmatic eruption of Okmok volcano, Aleutian Islands, Alaska: Chronology, deposits, and landform changes.

Le Corvec, N., Muirhead, J.D., White, J.D.L., 2018. Shallow magma diversions during explosive diatreme-forming eruptions. Nat. Commun. 9, 1–8. https://doi.org/10.1038/s41467-018-03865-x

Le Corvec, N., Spörli, K.B., Rowland, J., Lindsay, J., 2013. Spatial distribution and alignments of volcanic centers: Clues to the formation of monogenetic volcanic fields. Earth-Science Rev. 124, 96–114. https://doi.org/10.1016/j.earscirev.2013.05.005

Lesser y Asociados, S.A. de C.., 2000. Seguimiento del estudio hidrogeológico y modelo matemático del acuífero del Valle de Irapuato - Valle de Santiago - Huanímaro, Gto.

Lorenz, V., 2007. Syn- and posteruptive hazards of maar-diatreme volcanoes. J. Volcanol. Geotherm. Res. 159, 285–312. https://doi.org/10.1016/j.jvolgeores.2006.02.015

Lorenz, V., 2003. Maar- -Diatreme Volcanoes, their Formation, and their Setting in Hard-rock or Soft-rock Environments. Geolines 15, 5–10.

Lorenz, V., 1986. On the growth of maars and diatremes and its relevance to the formation of tuff rings. Bull. Volcanol. 48, 265–274.

Lorenz, V., 1974. Vesiculated tuffs and associated features. Sedimentology 21, 273–291. https://doi.org/10.1111/j.1365-3091.1974.tb02059.x

Losantos, E., Cebriá, J.M., Morán-Zenteno, D.J., Martiny, B.M., López-Ruiz, J., Solís-Pichardo, G., 2017. Petrogenesis of the alkaline and calcalkaline monogenetic volcanism in the northern sector of the Michoacán-Guanajuato Volcanic Field (Central Mexico). Lithos 288–289, 295–310. https://doi.org/10.1016/j.lithos.2017.07.013

Lozano-García, S., Ortega, B., Roy, P.D., Beramendi-Orosco, L., Caballero, M., 2015. Climatic variability in the northern sector of the American tropics since the latest MIS 3. Quat. Res. (United States) 84, 262–271. https://doi.org/10.1016/j.yqres.2015.07.002

Luhr, J.F., 2000. The geology and petrology of Volcan San Juan (Nayarit, Mexico) and the compositionally zoned Tepic Pumice. J. Volcanol. Geotherm. Res. 95, 109–156. https://doi.org/10.1016/S0377-0273(99)00133-X

Mahgoub, A.N., Böhnel, H., Siebe, C., Salinas, S., Guilbaud, M.N., 2017. Paleomagnetically inferred ages of a cluster of Holocene monogenetic eruptions in the Tacámbaro-Puruarán area (Michoacán, México): Implications for volcanic hazards. J. Volcanol. Geotherm. Res. 347, 360–370. https://doi.org/10.1016/j.jvolgeores.2017.10.004

Mazzarini, F., Ferrari, L., Isola, I., 2010. Self-similar clustering of cinder cones and crust thickness in the Michoacan-Guanajuato and Sierra de Chichinautzin volcanic fields, Trans-Mexican Volcanic Belt. Tectonophysics 486, 55–64. https://doi.org/10.1016/j.tecto.2010.02.009

McGee, L.E., Millet, M.A., Beier, C., Smith, I.E.M., Lindsay, J.M., 2015. Mantle heterogeneity controls on small-volume basaltic volcanism. Geology 43, 551–554. https://doi.org/10.1130/G36590.1

Mejía-Gómez, J.A., Sandoval-Minero, R., 2004. Uso del agua subterránea en la región acuífera Irapuato-Valle de Santiago (México) y su impacto sobre el sistema hidrogeológico. Bol. Geol. y Min. 115, 311–318.

Metcalfe, S.E., Leng, M.J., Kirby, J.R., Huddart, D., Vane, C.H., Gonzalez, S., 2016. Early–Mid Pleistocene environments in the Valsequillo Basin, Central Mexico: a reassessment. J. Quat. Sci. 31, 325–336. https://doi.org/10.1002/jqs.2851

Michon, L., Di Muro, A., Villeneuve, N., Saint-Marc, C., Fadda, P., Manta, F., 2013. Explosive activity of the summit cone of Piton de la Fournaise volcano (La Réunion island): A historical and geological review. J. Volcanol. Geotherm. Res. 264, 117–133. https://doi.org/10.1016/j.jvolgeores.2013.06.012

Morrisey, M., Zimanowski, B., Wohletz, K., Buetter, R., 2000. Phreatomagmatic fragmentation, in: Sigurdsson, H. (Ed.), Encyclopedia of Volcanoes. Academic Press, pp. 431–445.

Nakamura, K., Jacob, K.H., Davies, J.N., 1977. Volcanoes as possible indicators of tectonic stress orientation-Aleutians and Alaska. Pageoph, Birkhäuser Verlag, Basel 115, 87–112.

Nelson, S.A., González-Caver, E., 1992. Geology and K-Ar dating of the Tuxtla Volcanic Field, Veracruz, Mexico. Bull. Volcanol. 55, 85–96. https://doi.org/10.1007/BF00301122

Németh, K., Cronin, S.J., Smith, I.E.M., Agustin Flores, J., 2012. Amplified hazard of small-volume monogenetic eruptions due to environmental controls, Orakei Basin, Auckland Volcanic Field, New Zealand. Bull. Volcanol. 74, 2121–2137. https://doi.org/10.1007/s00445-012-0653-6

Németh, K., Kereszturi, G., 2015. Monogenetic volcanism: personal views and discussion. Int. J. Earth Sci. 104, 2131–2146. https://doi.org/10.1007/s00531-015-1243-6

Németh, K., Kósik, S., 2020. Review of explosive hydrovolcanism. Geosci. 10. https://doi.org/10.3390/geosciences10020044

Németh, K., White, J.D.L., 2003. Geochemical Evolution , Vent Structures , and Erosion History of Small-volume Volcanoes in the Miocene Intracontinental Waipiata Volcanic Field , New Zealand. Geolines 15, 89–92.

Nichols, C., Graettinger, A., 2021. The influence of regional stress and structural control on the shape of maar craters. Volcanica 4, 23–39. https://doi.org/10.30909/vol.04.01.2339

Nicholson, R.S., Gardner, J.E., Neal, C.A., 2011. Variations in eruption style during the 1931A.D. eruption of Aniakchak volcano, Alaska. J. Volcanol. Geotherm. Res. 207, 69–82. https://doi.org/10.1016/j.jvolgeores.2011.08.002

Ort, M.H., Carrasco-Núñez, G., 2009. Lateral vent migration during phreatomagmatic and magmatic eruptions at Tecuitlapa Maar, east-central Mexico. J. Volcanol. Geotherm. Res. 181, 67–77. https://doi.org/10.1016/j.jvolgeores.2009.01.003

Palladino, D.M., Valentine, G.A., Sottili, G., Taddeucci, J., 2015. Maars to calderas : end-members on a spectrum of explosive volcanic. Front. Earth Sci. 3, 1–8. https://doi.org/10.3389/feart.2015.00036

Pardo, M., Suarez, G., 1995. Shape of the subducted Rivera and Cocos plates in southern Mexico: seismic and tectonic implications. J. Geophys. Res. 100. https://doi.org/10.1029/95jb00919

Pasquaré, G., Vezzoli, L., Zanchi, A., 1987. Morphological and structural model of the Mexican Volcanic Belt. Geofis. Int. 26.

Pedrazzi, D., Kereszturi, G., Lobo, A., Geyer, A., Calle, J., 2020. Geomorphology of the post-caldera monogenetic volcanoes at Deception Island, Antarctica — Implications for landform recognition and volcanic hazard assessment. J. Volcanol. Geotherm. Res. 402, 106986. https://doi.org/10.1016/j.jvolgeores.2020.106986

Pedrazzi, D., Sunye-Puchol, I., Aguirre-Díaz, G., Costa, A., Smith, V.C., Poret, M., Dávila-Harris, P., Miggins, D.P., Hernández, W., Gutiérrez, E., 2019. The Ilopango Tierra Blanca Joven (TBJ) eruption, El Salvador: Volcano-stratigraphy and physical characterization of the major Holocene event of Central America. J. Volcanol. Geotherm. Res. 377, 81–102. https://doi.org/10.1016/J.JVOLGEORES.2019.03.006

Porter, S.C., 1972. Distribution, Morphology, and Size Frequency of Cinder Cones on Mauna Kea Volcano, Hawaii. Geol. Soc. Am. Bull. 83, 3607–3612.

Reimer, P.J., Austin, W.E.N., Bard, E., Bayliss, A., Blackwell, P.G., Bronk Ramsey, C., Butzin, M., Cheng, H., Edwards, R.L., Friedrich, M., Grootes, P.M., Guilderson, T.P., Hajdas, I., Heaton, T.J., Hogg, A.G., Hughen, K.A., Kromer, B., Manning, S.W., Muscheler, R., Palmer, J.G., Pearson, C., Van Der Plicht, J., Reimer, R.W., Richards, D.A., Scott, E.M., Southon, J.R., Turney, C.S.M., Wacker, L., Adolphi, F., Büntgen, U., Capano, M., Fahrni, S.M., Fogtmann-Schulz, A., Friedrich, R., Köhler, P., Kudsk, S., Miyake, F., Olsen, J., Reinig, F., Sakamoto, M., Sookdeo, A., Talamo, S., 2020. The IntCal20 Northern Hemisphere Radiocarbon Age Calibration Curve (0-55 cal kBP). Radiocarbon 62, 725–757. https://doi.org/10.1017/RDC.2020.41

Reyes-Guzmán, N., Siebe, C., Chevrel, M.O., Guilbaud, M.N., Salinas, S., Layer, P., 2018. Geology and radiometric dating of Quaternary monogenetic volcanism in the western Zacapu lacustrine basin (Michoacán, México): implications for archeology and future hazard evaluations. Bull. Volcanol. 80. https://doi.org/10.1007/s00445-018-1193-5

Reyes-Guzmán, N., Siebe, C., Chevrel, M.O., Pereira, G., Mahgoub, A.N., Böhnel, H., 2023. Holocene volcanic eruptions of the Malpaís de Zacapu and its pre-Hispanic settlement history. Anc. Mesoamerica 1759, 1–16. https://doi.org/10.1017/s095653612100050x

Rodríguez-Elizarrarás, S.R., Morales-Barrera, W. V., Pompa-Mera, V., Siebe, C., Benowitz, J., Layer, P.W., Lozano-Santacruz, R., Girón, P., 2023. Geochemistry and 40Ar/39Ar dating of the Sierra de Santa Marta in the tectonically controversial Los Tuxtlas Volcanic Complex (Veracruz, Mexico). J. South Am. Earth Sci. 124. https://doi.org/10.1016/j.jsames.2023.104250

Ross, P.S., Carrasco Núñez, G., Hayman, P., 2017. Felsic maar-diatreme volcanoes: a review. Bull. Volcanol. 79. https://doi.org/10.1007/s00445-016-1097-1

Santley, R.S., 2007. The prehistory of the Tuxtlas. UNAM Press.

Sheridan, M.F., Wohletz, K.H., 1983. Hydrovolcanism: Basic consideration and review. J. Volcanol. Geotherm. Res. 17, 1–29. https://doi.org/https://doi.org/10.1016/0377-0273(83)90060-4

Sheridan, M.F., Wohletz, K.H., 1981. Hydrovolcanic Explosions: The Systematics of Water-Pyroclast Equilibration. Science (80-.). 212, 1387–1389.

Siebe, C., 1986. On the possible use of cinder cones and maars as palaeoclimatic indicators in the closed basin of Serdán-Oriental, Puebla, México. J. Volcanol. Geotherm. Res. 28, 397–400. https://doi.org/10.1016/0377-0273(86)90034-X

Siebe, C., Macías, J.L., 2004. Volcanic hazards in the Mexico City metropolitan area from eruptions at Popocatépetl, Nevado de Toluca, and Jocotitlán stratovolcanoes and monogenetic scoria cones in the Sierra Chichinautzin Volcanic Field. Volcan. hazards Mex. City Metrop. area from eruptions Popocatépetl, Nevado Toluca, Jocotitlán Strat. monogenetic scoria cones Sierra Chichinautzin Volcan. F. https://doi.org/10.1130/2004.vhitmc.pfg

Siebe, C., Pereira, G., Dorison, A., Reyes-Guzmán, N., Ramírez-Uribe, I., Quezada-Ramírez, O., 2023. Fieldtrip guide: Arqueology and recent volcanism in the Zacapu lacustrine basin (Michoacan, Mexico), in: 80th Anniversary of Paricutín Volcano. Instituto de Geofísica, UNAM, Morelia.

Siebe, C., Salinas, S., 2014. Distribution of monogenetic phreato-magmatic volcanoes (maars, tuff cones, tuff rings) in the Mexican Volcanic Belt and their tectonic and hydrogeologic environment, in: IAVCEI – 5IMC. Querétaro, México, pp. 183–184.

Sieron, K., Francisco, S., Cerrillo, J., González, K., Francisco, Z., Montiel, C., Connor, C.B., Connor, L., Tapia, H., 2021. Morphology and distribution of monogenetic volcanoes in Los Tuxtlas Volcanic Field, Veracruz, Mexico: implications for hazard assessment. Bull. Volcanol. https://doi.org/10.1007/s00445-021-01467-y

Sieron, K., Siebe, C., 2008. Revised stratigraphy and eruption rates of Ceboruco stratovolcano and surrounding monogenetic vents (Nayarit, Mexico) from historical documents and new radiocarbon dates. J. Volcanol. Geotherm. Res. 176, 241–264. https://doi.org/10.1016/j.jvolgeores.2008.04.006

Smith, I.E.M., Németh, K., 2017. Source to surface model of monogenetic volcanism: A critical review. Geol. Soc. Spec. Publ. 446, 1–28. https://doi.org/10.1144/SP446.14

Sonder, I., Harp, A.G., Graettinger, A.H., Moitra, P., Valentine, G.A., Büttner, R., Zimanowski, B., 2018. Meter-Scale Experiments on Magma-Water Interaction. J. Geophys. Res. Solid Earth 123, 10,597-10,615. https://doi.org/10.1029/2018JB015682

Suter, M., López-Martínez, M., Quintero-Legorreta, O., Carrillo-Martínez, M., 2001. Quaternary intra-arc extension in the Central Trans-Mexican volcanic belt. Bull. Geol. Soc. Am. 113, 693–703. https://doi.org/10.1130/0016-7606(2001)113<0693:QIAEIT>2.0.CO;2

Unema, J.A., Ort, M.H., Larsen, J.F., Neal, C.A., Schaefer, J.R., 2016. Water-magma interaction and plume processes in the 2008 Okmok eruption, Alaska. Bull. Geol. Soc. Am. 128, 792–806. https://doi.org/10.1130/B31360.1

Ureta, G., Aguilera, F., Vilches, M., 2020. An Overview of the Mafic and Felsic Monogenetic Neogene to Quaternary Volcanism in the Central Andes, Northern Chile (18-28°Lat.S), in: Updates in Volcanology-Transdisciplinary Nature of Volcano Science. https://doi.org/10.5772/intechopen.93959

Uribe-Cifuentes, R.M., Urrutia-Fucugauchi, J., 1999. Paleomagnetic study of the Valle de Santiago volcanics, Michoacan-Guanajuato volcanic field, Mexico. Geofis. Int. 38, 217–230. https://doi.org/10.22201/igeof.00167169p.1999.38.4.504

Urrutia-Fucugauchi, J., González-Morán, T., 2006. Structural pattern at the northwestern sector of the Tepic-Zacoalco rift and tectonic implications for the Jalisco block , western Mexico. Earth, planets Sp. 58, 1303–1308.

Valentine, G.A., White, J.D.L., Ross, P.S., Graettinger, A.H., Sonder, I., 2017. Updates to Concepts on Phreatomagmatic Maar-Diatremes and Their Pyroclastic Deposits. Front. Earth Sci. 5, 1–7. https://doi.org/10.3389/feart.2017.00068

Vázquez-Selem, L., Heine, K., 2011. Late Quaternary Glaciation in Mexico, in: Developments in Quaternary Science. pp. 849–861. https://doi.org/10.1016/B978-0-444-53447-7.00061-1

Verma, S.P., 2006. Extension-related origin of magmas from a garnet-bearing source in the Los Tuxtlas volcanic field, Mexico. Int. J. Earth Sci. 95, 871–901. https://doi.org/10.1007/s00531-006-0072-z

Waters, A.C., Fisher, R. V., 1971. Base surges and their deposits: Capelinhos and Taal Volcanoes. J. Geophys. Res. 76, 5596–5614. https://doi.org/10.1029/jb076i023p05596

White, J.D.L., 1991. Maar-diatreme phreatomagmatism at Hopi Buttes, Navajo Nation (Arizona), USA. Bull. Volcanol. 53, 239–258. https://doi.org/10.1007/BF00414522

White, J.D.L., Ross, P.S., 2011. Maar-diatreme volcanoes: A review. J. Volcanol. Geotherm. Res. 201, 1–29. https://doi.org/10.1016/j.jvolgeores.2011.01.010

Wohletz, K.H., 1986. Explosive magma-water interactions: Thermodynamics, explosion mechanisms , and field studies. Bull. Volcanol. 48, 245–264.

Wohletz, K.H., 1983. Mechanisms of hydrovolcanic pyroclastic foration: Grain-size, scanning electron microscopy, and experimental studies. J. Volcanol. Geotherm. Res. 17, 31–63.

Wohletz, K.H., Sheridan, M.F., 1983. Hydrovolcanic explosions II. Evolution of basaltic tuff rings and tuff cones. Am. J. Sci. 283, 385–413.

Wood, C.A., 1980. Morphometric analysis of cinder cone degradation. J. Volcanol. Geotherm. Res. 8, 137–160. https://doi.org/10.1016/0377-0273(80)90101-8